AEROSPACE REPORT NO.
TOR-0086(6728-01)-3

Contract No. N00014-81-MP-10006; NR-4313279

# Mesophase Behavior Fundamental to the Processing of Carbon-Carbon Composites

Prepared by

J. L. WHITE and P. M. SHEAFFER
Materials Sciences Laboratory



3 June 1986

Interim Technical Report for
Period 1 October 1984 through 30 September 1985

Prepared for
OFFICE OF NAVAL RESEARCH
800 North Quincy Street
Arlington, VA 22217





Laboratory Operations
THE AEROSPACE CORPORATION

## LABORATORY OPERATIONS

The Aerospace Corporation functions as an "architect-engineer" for national security projects, specializing in advanced military space systems. Providing research support, the corporation's Laboratory Operations conducts experimental and theoretical investigations that focus on the application of scientific and technical advances to such systems. Vital to the success of these investigations is the technical staff's wide-ranging expertise and its ability to stay current with new developments. This expertise is enhanced by a research program aimed at dealing with the many problems associated with rapidly evolving space systems. Contributing their capabilities to the research effort are these individual laboratories:

Aerophysics Laboratory: Launch vehicle and reentry fluid mechanics, heat transfer and flight dynamics; chemical and electric propulsion, propellant chemistry, chemical dynamics, environmental chemistry, trace detection; spacecraft structural mechanics, contamination, thermal and structural control; high temperature thermomechanics, gas kinetics and radiation; cw and pulsed chemical and excimer laser development including chemical kinetics, spectroscopy, optical resonators, beam control, atmospheric propagation, laser effects and countermeasures.

Chemistry and Physics Laboratory: Atmospheric chemical reactions, atmospheric optics, light scattering, state-specific chemical reactions and radiative signatures of missile plumes, sensor out-of-field-of-view rejection, applied laser spectroscopy, laser chemistry, laser optoelectronics, solar cell physics, battery electrochemistry, space vacuum and radiation effects on materials, lubrication and surface phenomena, thermionic emission, photosensitive materials and detectors, atomic frequency standards, and environmental chemistry.

Computer Science Laboratory: Program verification, program translation, performance-sensitive system design, distributed architectures for spaceborne computers, fault-tolerant computer systems, artificial intelligence, microelectronics applications, communication protocols, and computer security.

Electronics Research Laboratory: Microelectronics, solid-state device physics, compound semiconductors, radiation hardening; electro-optics, quantum electronics, solid-state lasers, optical propagation and communications; microwave semiconductor devices, microwave/millimeter wave measurements, diagnostics and radiometry, microwave/millimeter wave thermionic devices; atomic time and frequency standards; antennas, rf systems, electromagnetic propagation phenomena, space communication systems.

Materials Sciences Laboratory: Development of new materials: metals, alloys, ceramics, polymers and their composites, and new forms of carbon; nondestructive evaluation, component failure analysis and reliability; fracture mechanics and stress corrosion; analysis and evaluation of materials at cryogenic and elevated temperatures as well as in space and enemy-induced environments.

Space Sciences Laboratory: Magnetospheric, auroral and cosmic ray physics, wave-particle interactions, magnetospheric plasma waves; atmospheric and ionospheric physics, density and composition of the upper atmosphere, remote sensing using atmospheric radiation; solar physics, infrared astronomy, infrared signature analysis; effects of solar activity, magnetic storms and nuclear explosions on the earth's atmosphere, ionosphere and magnetosphere; effects of electromagnetic and particulate radiations on space systems; space instrumentation.

AD-A174 934

-- 5 - CORPORATE AUTHOR: AEROSPACE CORP EL SEGUNDO CA MATERIALS SCIENCES
-- LAB
-- 6 - UNCLASSIFIED TITLE: MESOPHASE BEHAVIOR FUNDAMENTAL TO THE
-- PROCESSING OF CARBON-CARBON COMPOSITES.
-- 9 - DESCRIPTIVE NOTE: INTERIM REPT., 1 OCT 84 - 30 SEP 85,

--10 - PERSONAL AUTHORS: WHITE,J. L. ;SHEAFFER,P. M. ;
--11 - REPORT DATE: JUN 03, 1986
--12 - PAGINATION: 60P
--14 - REPORT NUMBER: TOR-0086(6728-01)-3
--15 - CONTRACT NUMBER: N00014-81-MP-10000
--16 - MONITOR ACRONYM: ONR
--19 - MONITOR SERIES: 4313279
--20 - REPORT CLASSIFICATION: UNCLASSIFIED
--22 - LIMITATIONS (ALPHA): APPROVED FOR PUBLIC RELEASE; DISTRIBUTION
-- UNLIMITED. [redacted]
-- [redacted]
--30 - LIMITATION CODES: 1
--******
-- END OF DISPLAY LIST

-- <<ENTER NEXT COMMAND>>

Alt-Z FOR HELP 3 ANSI 3 HDX 3 3 LOG CLOSED 3 PRINT OFF 3 PARITY

Aerospace Report No.
TOR-0086(6728-01)-3

Contract No. N00014-81-MP-10006; NR-4313279

# MESOPHASE BEHAVIOR FUNDAMENTAL TO THE PROCESSING OF CARBON-CARBON COMPOSITES

Prepared by

J. L. White and P. M. Sheaffer
Materials Sciences Laboratory

3 June 1986

Laboratory Operations
THE AEROSPACE CORPORATION
El Segundo, CA 90245

Interim Technical Report for
Period 1 October 1984 through 30 September 1985

Prepared for

OFFICE OF NAVAL RESEARCH
800 North Quincy Street
Arlington, VA 22217

Aerospace Report No.
TOR-0086(6728-01)-3

MESOPHASE BEHAVIOR FUNDAMENTAL TO THE
PROCESSING OF CARBON-CARBON COMPOSITES
Interim Technical Report for Period
1 October 1984 through 30 September 1985

Prepared

J. L. White

P. M. Sheaffer

Approved

H. A. Katzman, Head
Carbon and Polymers Department

R. W. Fillers, Director
Materials Sciences Laboratory

The information in a Technical Operating Report is developed for a particular program and is therefore not necessarily of broader technical applicability.

# FOREWORD

This is the fourth annual report on a program to study the fundamentals of mesophase behavior that pertain to the processing of carbon-fiber-reinforced carbon-matrix composites. The work is supported by the Office of Naval Research (ONR) under Contract No. N00014-81-MP-10006, work unit number NR-4313279. The principal investigator is J. L. White. The ONR scientific officer is L. H. Peebles, Jr.; his interest and support are gratefully acknowledged. We also thank J. S. Evangelides and G. S. Rellick for criticism and consultation.

ABSTRACT

The behavior of the carbonaceous mesophase under conditions of composite fabrication has been investigated to understand (1) the formation of microstructure within the fiber matrix, (2) the mechanisms that determine process efficiency, and (3) how the properties of the matrix are affected by carbonizing and graphitizing heat treatments. Experimental work in FY 85 focused on two concepts to introduce new approaches to fabrication: pressure cycling, while the mesophase is still plastic, to attain more complete impregnation; and oxidation stabilization, to circumvent the inefficiencies of thermal hardening caused by blowout of the mesophase matrix by gaseous pyrolysis products. Other experimental work included observations of the microstructural mechanisms operating in the mesophase matrix during heat treatment beyond the point of mesophase hardening.

Pressure Cycling for Improved Impregnation

Working with A240 petroleum pitch, we found high-pressure pyrolysis conditions about 460°C for a heating rate of 10°C/h and pressure of 15 kpsi where the pitch had transformed to a mesophase but was still deformable within a 3D preform. Pressure cycling near 460°C, from 15 to 1 kpsi and return, produced density levels of as high as 1.5 g/cm$^3$ in the first impregnation. Microscopic examination showed good filling of fiber bundles and weave cavities to depths of about 5 mm.

Oxidation Stabilization

Working with drawn mesophase rods, we achieved oxidation stabilization to depths of 70 μm from a free surface or from cracks with access to the oxidizing atmosphere. Thermogravimetric analysis (TGA) measurements of oxidation (over 220 to 320°C) and subsequent carbonization have shown that the lower temperature levels for oxidation offer better carbon yields and ensure stabilization of microstructure. Four tests of oxidation stabilization were applied to preforms impregnated by pressure cycling. They demonstrated that oxidation levels of 5 to 11% can be attained in bodies of about 8 mm in

thickness. In one test, the pitch was only partially transformed to mesophase, and the oxidation process stabilized both the isotropic pitch and the mesophase. However, reduced oxidation rates were measured for the most fully impregnated specimens, and more lengthy oxidation exposures may be necessary to attain stabilization throughout the composite.

Effects of Heat Treatment on Mesophase Matrices

In micrographic observations on singly impregnated fiber bundles and 3D preforms heat treated to 1200 and 1700°C, the mesophase distortions within a preform were found to be similar to those observed in earlier work on calcined coke. The fold-sharpening mechanism operating on the curved layers of a sheath around a filament causes extensive debonding and the localization of load transfer between filament and matrix. The matrix distortions can be so large that some filaments are damaged by longitudinal splitting.

CONTENTS

FIGURES

FIGURES (Continued)

TABLES

# I. INTRODUCTION

Carbon-fiber-reinforced carbon-matrix composites are now finding wider-ranging applications, e.g., as biomedical implants, although the major impetus for their further development continues to come from space and defense requirements, for which their cost is justified by unique capabilities of thermal and mechanical performance. The fabrication processes often involve the formation of a pregraphitic matrix by impregnating a fiber preform with organic materials that pass through a mesophase (liquid crystal) state upon carbonization. The carbonaceous mesophase then plays a key role not only in ensuring the graphitizability of the matrix but also by determining, through its behavior, the matrix microstructure and the processing strategies that can be used to attain desired density levels.

From a scientific viewpoint, mesophase microstructures form by structural mechanisms acting either in the liquid-crystalline state or in the liquid-crystalline glass that results from thermally or chemically hardening the mesophase. This research has addressed such basic phenomena as wetting behavior of mesophase-bearing liquids, molecular alignment on mesophase-wetted substrates, disclination interactions, and graphitization mechanisms commencing from the state of organization of carbon in just-hardened mesophase, i.e., the mesophase glass described in practical terms as coke or semi-coke. Section II contains an overview of these phenomena.

From a composite-fabrication viewpoint, the carbonaceous mesophase is a viscous reactive liquid in the practical ranges of processing variables, and the gaseous reaction products cause bloating that seriously reduces densification efficiency. Our experimental efforts in FY 85 included exploratory work on two modifications to conventional processing: pressure cycling while the mesophase is fluid to achieve more complete impregnation (described in Section III), and oxidation stabilization as an alternative to thermal hardening to fix the mesophase in place within the fiber preform (discussed in Section IV).

## II. MICROSTRUCTURE FORMATION IN COMPOSITE PROCESSING

The formation of mesophase microstructures within the fiber bundles of a carbon-carbon composite has been treated in previous reports[1-3] and summarized in a recent paper[4] for the JANNAF Rocket Nozzle Technology Subcommittee. Our observations, most extensively on fiber bundles impregnated with a petroleum pitch (Ashland A240) but also on bundles in a coal-tar pitch (Allied 15V), reflected consistent patterns of microstructure formation that were independent of fiber type and process pressure. Here, we present observations on longitudinal sections (not documented in previous reports) and offer two schematic diagrams that summarize the wetting and alignment behavior dominating microstructure formation for all the cases that we have studied.

Our previous reports have presented only transverse views of fiber bundles, simply because longitudinal sections are much more difficult to polish to the standard desired for publication-quality micrographs. The difficulties are most serious at early stages in the mesophase transformation, when the delicate mesophase can be damaged or destroyed as some filaments loosen and move locally under polishing stress. Two longitudinal views relatively free of polishing damage are illustrated in Fig. 1 for a 3D pressure-cycled composite that is detailed further in Section III. Features of the polarized-light micrographs are as follows:

- Elongated mesophase droplets formed on fiber substrates.
- Deformed mesophase bridging the gap between filaments; the deformation is attributed to bubble motion during pressure cycling.
- Bright ribbons, banded with an extinction contour and lying between filaments; this feature implies the presence of a $-2\pi$ wedge disclination with a continuous core.[5]

Mesophase wetting and alignment conditions on carbon filaments are illustrated in Fig. 2 for the early stages of mesophase transformation observed in both petroleum and coal-tar pitches. The elongated mesophase droplets have been present even when pressure cycling has not occurred; the elongation may be the natural growth behavior on the fiber substrate rather

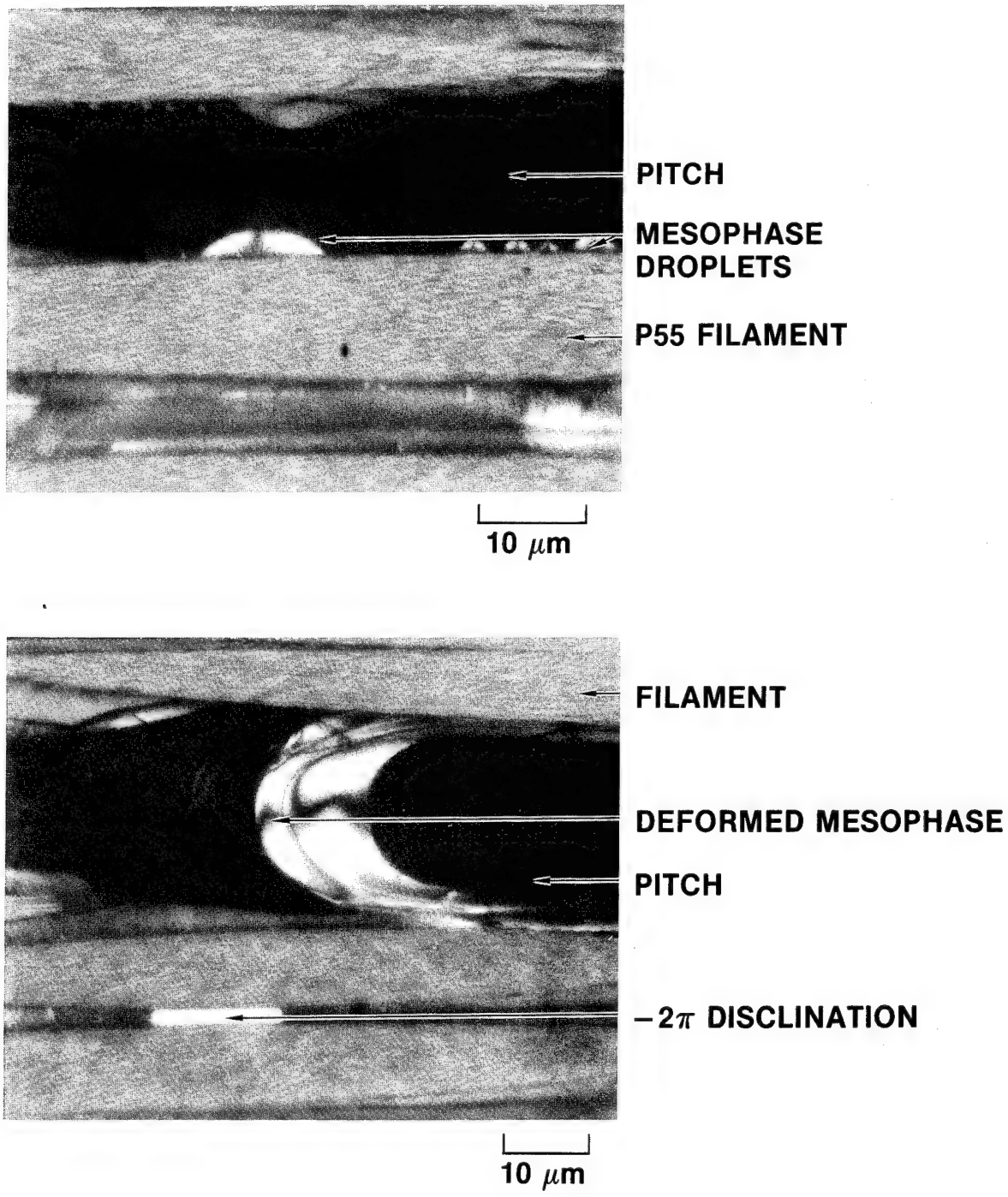


Figure 1. Longitudinal Views of Mesophase Formation in Fiber Bundles. 3D composite MC18C pressure-cycled under conditions given in Table 1. Crossed polarizers, oil immersion.

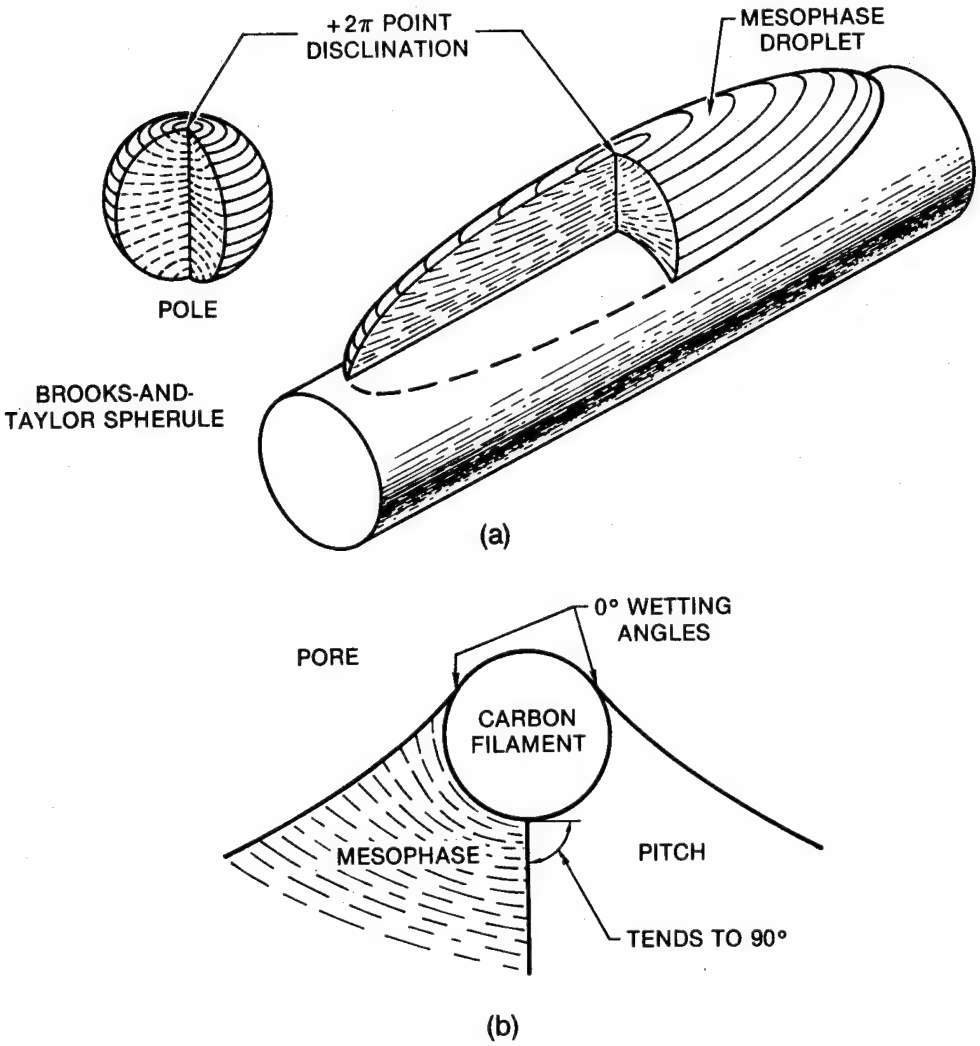


Figure 2. Wetting and Alignment Conditions for Mesophase on Carbon Fiber: (a) Mesophase droplets precipitated from pitch, sectioned to show internal structure. (b) Wetting and alignment for a filament at a bubble pore. From Ref. 4.

than a result of deformation. The internal structure of the droplet resembles a Brooks-and-Taylor spherule[6] extended in one dimension, the mesophase layers adjacent to the filament lying parallel to the cylindrical surface and with a partial $+2\pi$ point disclination on the periphery of the droplet.

At pores or interfaces with pitch, the mesophase layers stand normal to the interfaces, at least as long as the mesophase remains quite fluid. Near carbon filaments, the mesophase layers exhibited sheathlike parallel alignment at all stages of pyrolysis. The tendency for the pitch-mesophase interface to be oriented near normal to the filament surface implies a close balance between the wetting energies of pitch and mesophase on the carbon filament. The normal orientation of the interface corresponds to the equilibrium alignments of the mesophase layers at the pitch and filament interfaces. At bubble pores in the fiber bundles, both pitch and mesophase display near-zero wetting angles on the filament substrates. Along the pore-mesophase-filament line, there is an ambiguity in layer orientation that cannot be resolved by polarized light microscopy.

Thus, as far as wetting and wicking effects are concerned, the mesophase-ordering transformation sweeps through the pitch matrix with little or no disturbance. However, the alignment of mesophase layers parallel to the filament surface, as illustrated by Fig. 3, is the dominant mechanism for determining the microstructure in graphitizable matrices of fiber bundles. Even in the presence of magnetic fields sufficiently strong to reorient the bulk mesophase, the layers along the fiber surfaces retain their sheathlike orientation.

The matrix disclinations within a fiber bundle can be readily predicted, therefore, from the geometry of filaments surrounding each matrix channel. Since the sheath surrounding each filament constitutes a $+2\pi$ disclination, the additivity rule for disclinations[8] requires that the matrix contain primarily the $-\pi$ and $-2\pi$ disclinations sketched in Fig. 3. Note that the $-2\pi$ disclinations, which occur preferentially in matrix channels bounded by four filaments in a square array, can detract from the matrix's contribution to the longitudinal elastic modulus because their continuous cores tilt the stiff graphitic layers out of parallel alignment with the filaments.[9]

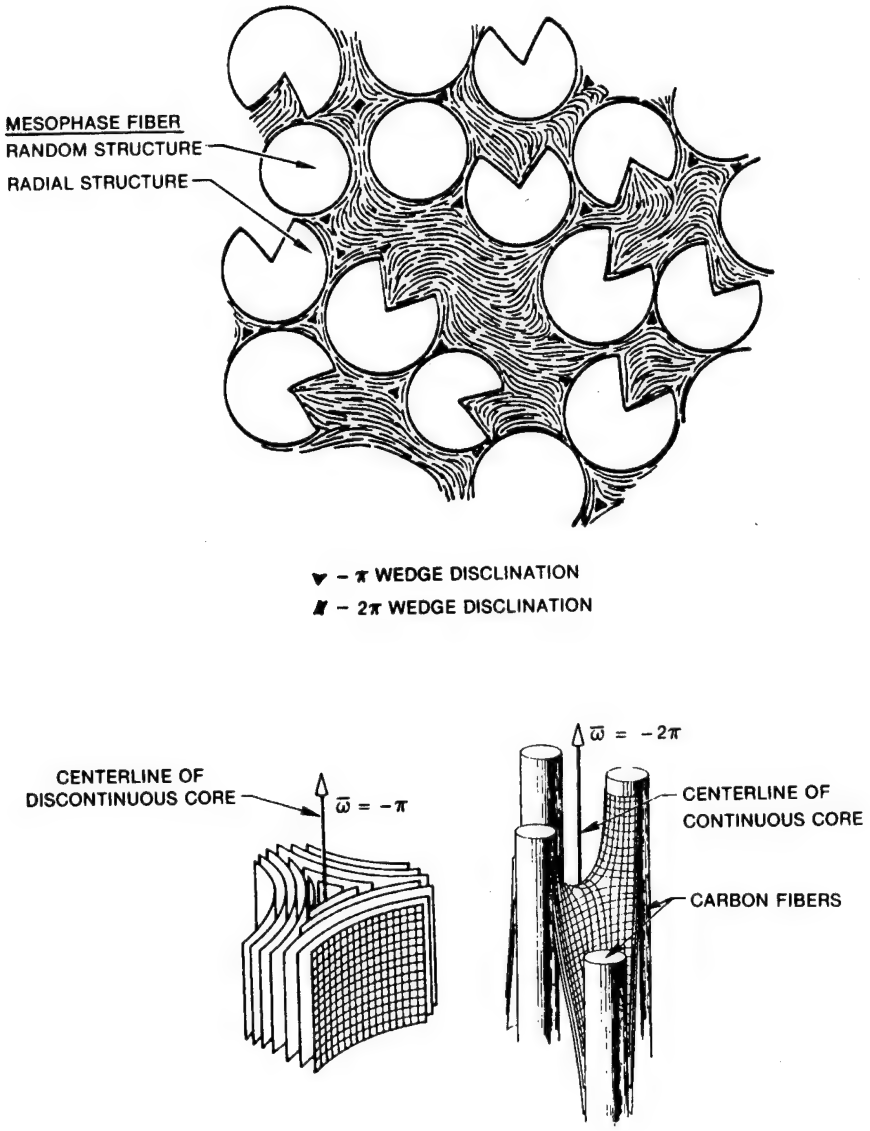


Figure 3. Mesophase Alignment within a Fiber Bundle. Mesophase pitch fiber (VSA-11) in A240 petroleum pitch. Mesophase layer orientations mapped by polarized-light micrography.[5] Sketches of the $-\pi$ and $-2\pi$ disclinations that predominate in the matrix are included to show the difference in layer orientations within the disclination cores.

## III. MESOPHASE IMPREGNATION BY PRESSURE CYCLING

Evangelides and Meyer[10] have shown that conventional multiple-cycle high-pressure impregnation and densification processes are inefficient relative to the pyrolysis yields expected at high pressure. A basic difficulty in conventional processing stems from reliance on pyrolytic reactions for both matrix hardening and mesophase formation, reactions that produce gases of low critical point, principally $CH_4$ and $H_2$. The resultant bubble nucleation and percolation is responsible for the extensive bloating and deformation that is well known in practical pyrolysis processes such as petroleum coking.[11] Micrographic evidence was given in the last annual report[3] that bloating during composite processing also produces appreciable porosity, even under 15,000-psi applied pressure, and thus prevents the attainment of full impregnation at the critical stage of mesophase hardening.

With this background, we can define an approach to improved processing of composites with graphitic matrices. The matrix precursor should first be transformed to mesophase pitch, then manipulated while still fluid to fill the composite body, leaving as little bubble porosity as possible, and finally hardened in place by a means that avoids bloating or other destructive effects when the composite is carbonized. Two processes that may meet these needs for 3D composites are:

- Pressure cycling, which flushes pyrolysis bubbles from the fiber bundles and weave cavities after the impregnant has been transformed to mesophase and while it is still fluid, thus producing an unhardened but more thoroughly impregnated composite body with the matrix in the desired mesophase state.

- Oxidation stabilization, which fixes the mesophase matrix in place, thus avoiding bloating effects in further heat treatment.

This section reports on experiments to test the pressure-cycling concept. Section IV describes work on mesophase oxidation within 3D fiber preforms.

Measurements of the effect of high-pressure pyrolysis on the softening and hardening points of mesophase produced from A240 petroleum pitch were included in the previous annual report.[3] (The hardening point is defined as

the processing temperature at which a pyrolysis residue has just hardened, e.g., no longer displays a softening point in a penetrometer test.) For a heating rate of 10°C/h, a pyrolysis pressure of 15,000 psi caused a sharp decrease in softening point and a modest increase in hardening point, thus opening a temperature range near 470°C within which the mesophase matrix may be manipulated by varying the applied pressure. With the concept of pressure cycling, we can envisage the use of pressure decreases from, say, 15,000 to 1000 psi, to expand bubbles sufficiently to free them from the composite. This decompression is followed by reapplying full pressure so that surrounding mesophase is forced into the composite. It may be desirable to repeat this cycle to work bubbles from the interior of a composite.

Our objective and approach relate closely to those of Brückmann,[12,13] who sought to produce more fully impregnated unidirectional fiber bundles by utilizing mesophase deformability. Working with a coal-tar pitch, Brückmann[13] found a region near 460°C in room-pressure thermal treatment where the pitch was fully transformed to mesophase and still deformable. He applied mechanical pressures up to 2200 psi to compress mesophase-impregnated fiber bundles while heating at rates of about 7°C/min. Appreciable transverse shrinkage, of the order of 30%, took place at 460°C. The unidirectional fiber bundles were hardened by continued heating under the transverse mechanical restraint. Optical micrography indicated full impregnation, and densities of 1.70 to 1.72 $g/cm^3$ (after thermal treatment to 670°C) were attained in bundles of P55 carbon fiber.

In the present work, we seek to extend to 3D composites the concept of densification by mesophase flow, using hydraulic pressure applied by an inert cover gas. The goal in the pressure-cycling step is to achieve a more fully mesophase-impregnated preform since we foresee the total process as including oxidation stabilization prior to carbonizing heat treatment. Thus, after the impregnation step is completed at temperatures at which the mesophase is deformable, the composite specimen is cooled to minimize bloating reactions.

Four pressure-cycling experiments have been run under the conditions summarized in Table 1, using mesophase produced <u>in situ</u> from A240 petroleum

Table 1. Mesophase Impregnation by Pressure Cycling

| Precursor: A240 Petroleum Pitch | | | | | |
|---|---|---|---|---|---|
| Run Designation | | MC18A | MC18B | MC18C | MC18D |
| Pyrolysis Conditions | | | | | |
| Heating rate | (°C/h) | 10.1 | 9.3 | 10.0 | 10.0 |
| Maximum temperature | (°C) | 464 | 466 | 456 | 460 |
| Hold time at $T_{max}$ (prior to pressure cycling) | (min) | 78 | ~ 30 | 0 | 0 |
| Pressure-Cycle Temperatures | | | | | |
| Depressurization | (°C) | 460 ± 8 | 456 ± 4 | 460 ± 22 | 463 ± 4 |
| Repressurization | (°C) | 454 ± 10 | 453 ± 10 | 460 ± 22 | 463 ± 4 |
| Results | | | | | |
| Composite density | ($g/cm^3$) | 1.19 | 1.36 | 1.52 | 1.47 |
| Matrix wt. fraction | (Note a) | 0.287 | 0.377 | 0.442 | 0.421 |
| Yield | (%) | 71 | 64 | 63 | NA |
| Transformation extent | (Note b) | near-100% | near-100% | incomplete | over 90% |
| Comments | | Note c | Note d | Note e | |

NA = Not available.

NOTES:

[a]Calculated with preform density = 0.85 $g/cm^3$.

[b]Visual estimates from micrographs.

[c]Pitch charge was inadequate to immerse preform.

[d]Power failure just prior to reaching maximum pyrolysis temperature; proceeded with run despite strong thermal disturbance.

[e]Strong temperature cycling during pressure cycle.

pitch. The runs were made in a low-thermal-inertia furnace operating in a cold-wall autoclave to permit rapid thermal response during pressure changes and quenching. The preform specimens were cylindrical, approximately 16 mm in diameter and 20 mm in height, as excised from a P55 carbon fiber 3D preform supplied to Aerospace by the Naval Surface Weapons Center.[14] Each preform cylinder was encased in a metal cage, then placed in an aluminum test tube and covered with 15 g of crushed pitch. The pressure-temperature record for the fourth pressure-cycling experiment, given in Fig. 4, presents the time scale for the pressure cycle and indicates the apparatus performance. Temperature upsets occur during pressure changes but appear to be manageable. The low end of the pressure cycle was set at 1000 psi to avoid contributions to bubble volume by heavy volatiles. Short cycle times of about 15 min were used to minimize viscosity increases during the pressure cycle.

The density results in Table 1 are generally higher than the values of 1.25 to 1.29 $g/cm^3$ reported by Seibold et al.[15] for the first cycle of conventional high-pressure processing (values measured after pressurized thermal treatment to 650°C). Although Brückmann's values[13] of 1.70 to 1.72 $g/cm^3$ (after thermal treatment to 670°C) are not directly comparable because his unidirectional composites lack the weave cavities of 3D composites, they do suggest the gains to be made if full impregnation can be achieved. Useful improvements in densification were not achieved in the initial pressure-cycling experiments MC18A and MC18B. Reasoning that the mesophase produced was too viscous to respond to the pressure cycle, we used less severe pyrolysis conditions in experiments MC18C and MC18D, in which density levels of about 1.5 $g/cm^3$ were attained.

The composites were examined microscopically on full vertical sections that included the axes of the cylindrical specimens. For comparison, Fig. 5 illustrates the microstructure of a composite prepared from the same preform but without pressure cycling: There is little filling of weave cavities at any point in the specimen, and there is appreciable porosity within the fiber bundles.

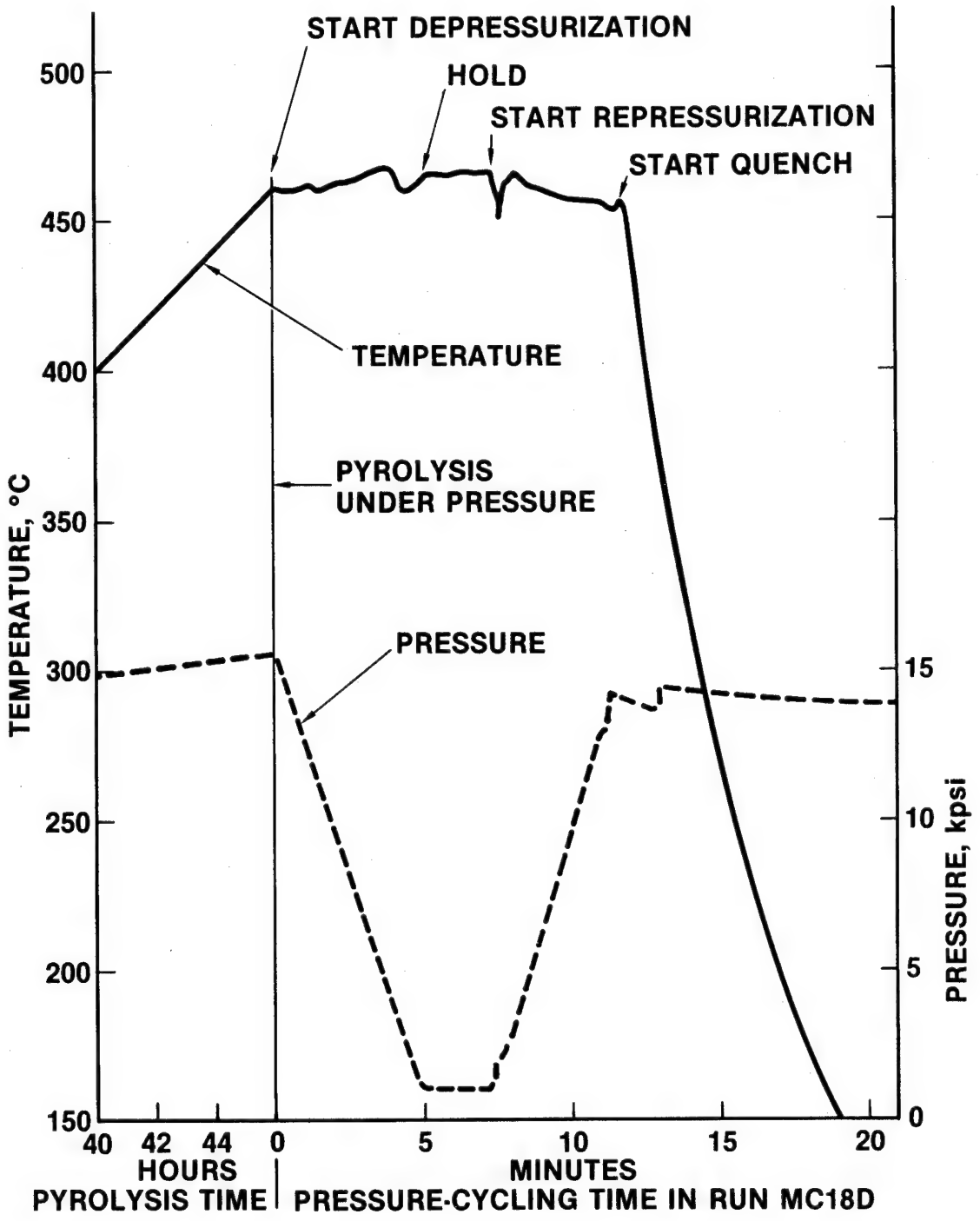


Figure 4. Temperature and Pressure Records for a Pressure-cycling Run

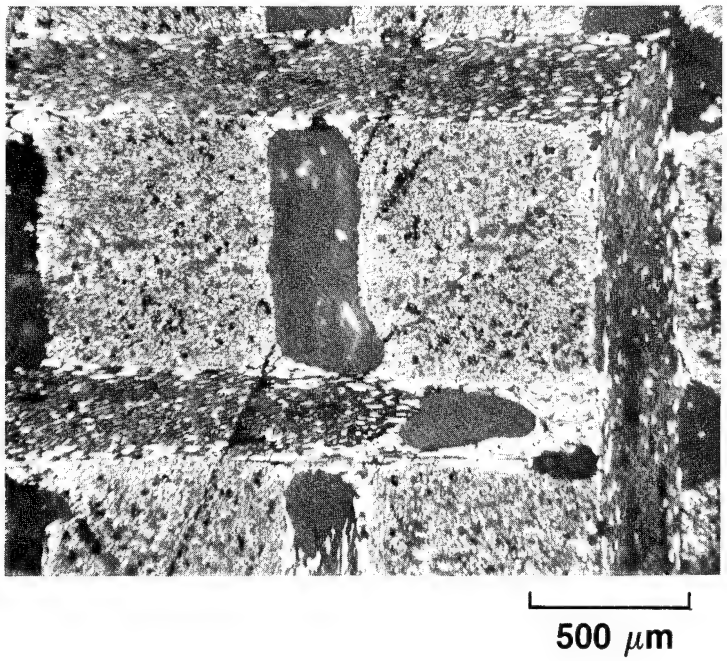


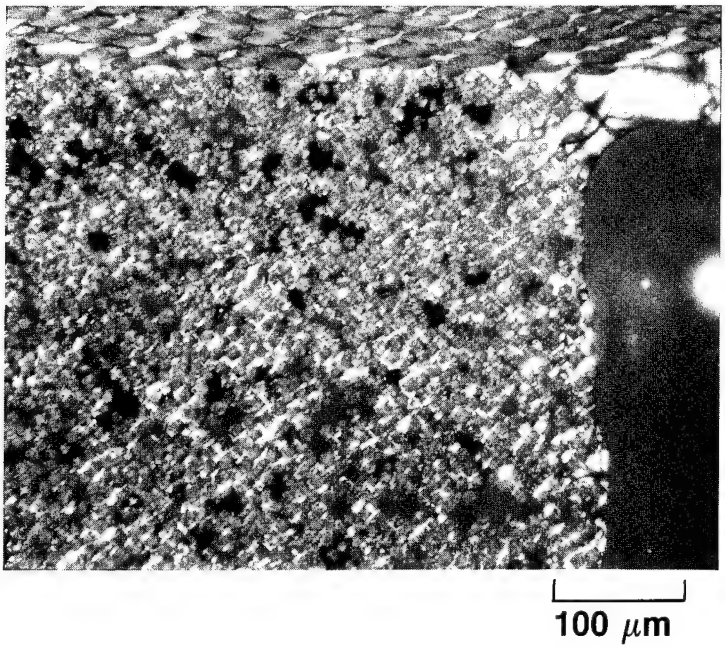


Figure 5. Microstructure of a 3D Composite Prepared by High-Pressure Pyrolysis without Pressure Cycling. P55 fiber preform pyrolyzed under A240 petroleum pitch to 496°C at 11°C/h and 15 kpsi. Partially crossed polarizers.

The degree of densification achieved with pressure cycling in experiment MC18C is illustrated in the micrographs of Fig. 6. Although impregnation was satisfactory for both bundles and weave cavities to a depth of about 5 mm, the transformation to mesophase was incomplete and there were appreciable fractions of untransformed pitch in most of the weave cavities. The fiber bundles were well impregnated throughout the composite, although small pools of untransformed pitch and occasional pores were observed in most bundles.

The densification achieved in experiment MC18D is depicted in the micrographs of Figs. 7 and 8. Although the mesophase transformation was almost complete, some small regions of pitch can be found in most fiber bundles and in weave cavities. The extent of cavity impregnation decreased from the edge to the center of the preform. Figure 7 includes micrographs taken at two levels along the cylindrical axis to illustrate the range of cavity filling observed. Figure 8 gives higher-magnification views of a fiber bundle from a region where the weave cavities were poorly filled; nevertheless, the adjacent fiber bundles were much better filled than in the specimen of Fig. 5.

At this stage the results of the pressure-cycling experiments appear promising but incomplete because the process variables must still be explored. However, the mesophase-impregnated preforms provided suitable specimens for testing the concept of oxidation stabilization for 3D composites.

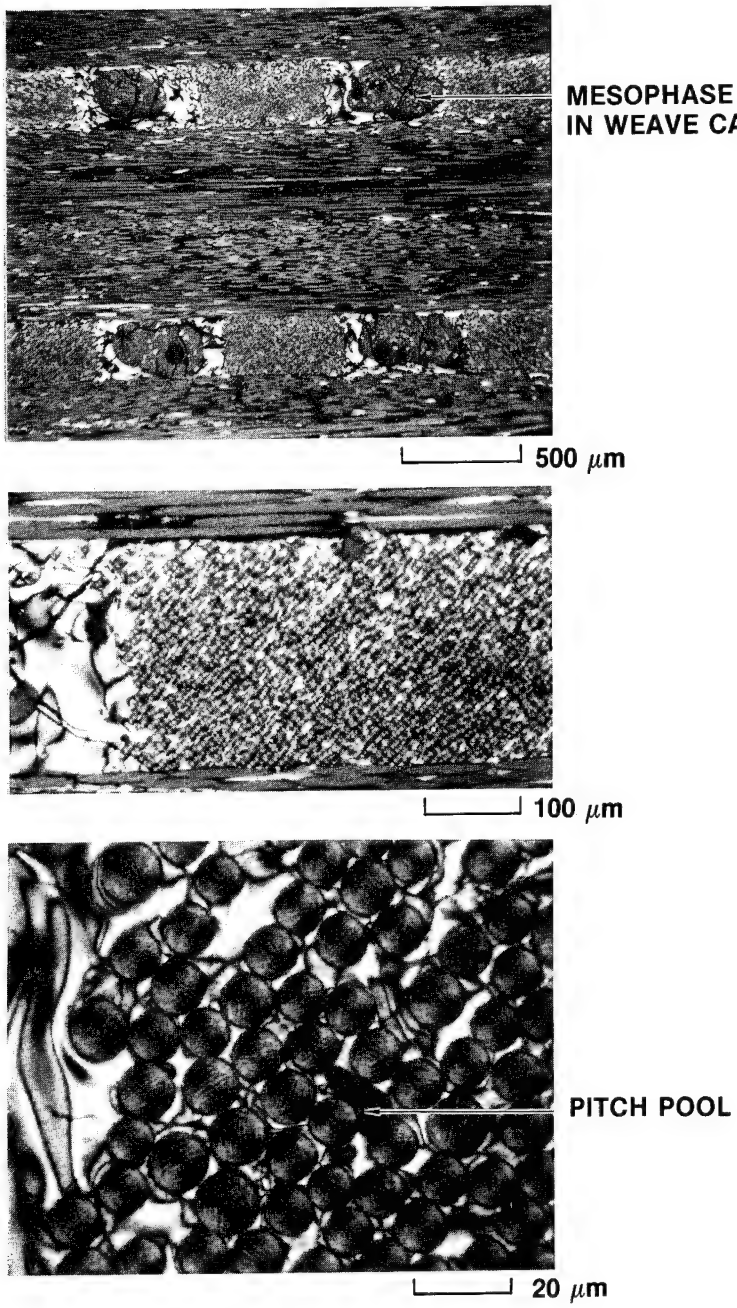


Figure 6. Microstructure of a 3D Composite Prepared by Pressure Cycling. Specimen from experiment MC18C, observed at a depth of 2 mm from cylindrical surface. Crossed polarizers.

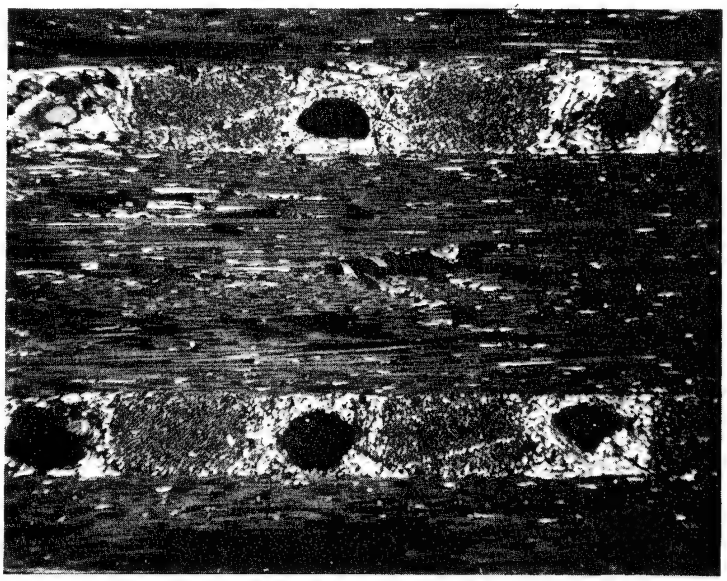


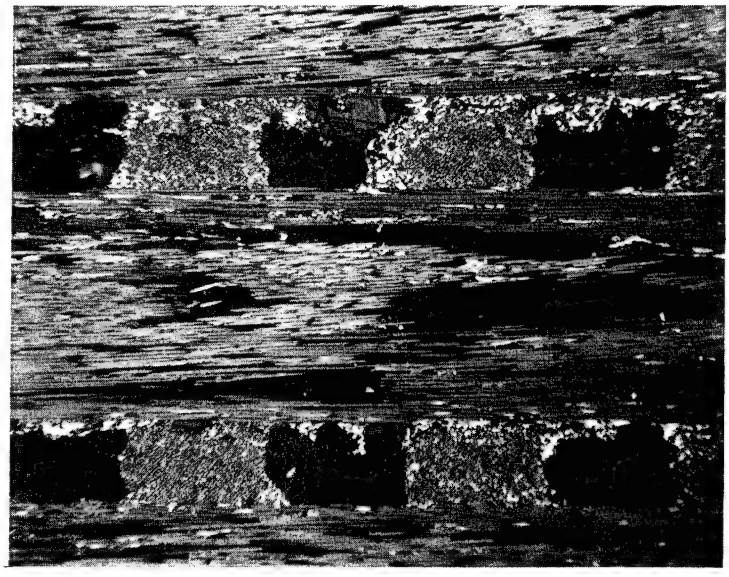


Figure 7. Variations in Filling of Weave Cavities in a Pressure-cycled Specimen. Specimen from experiment MC18D, examples of (a) well-filled weave cavities and (b) poorly filled cavities. Partially crossed polarizers.

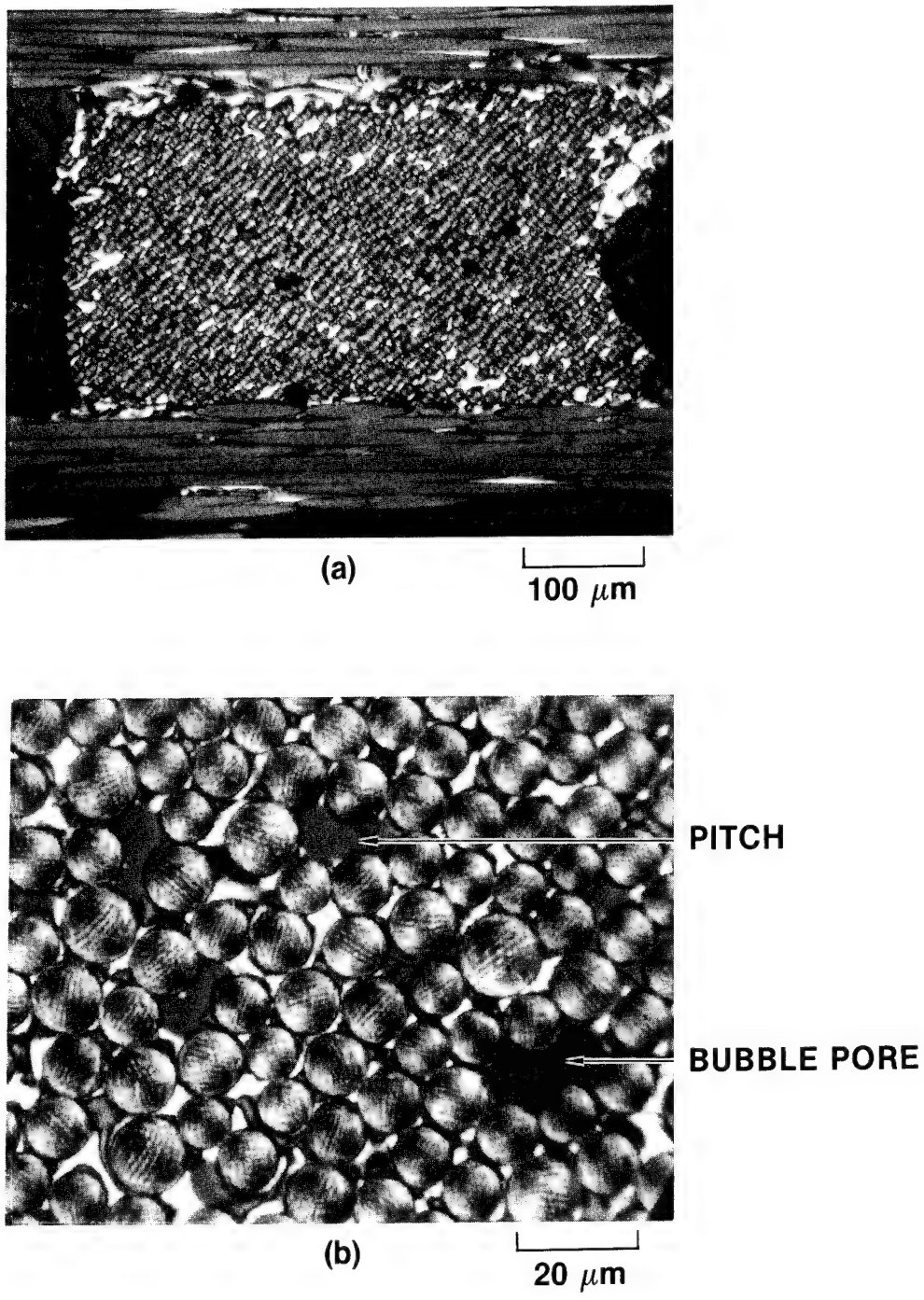


Figure 8. Fiber Bundle in a Pressure-cycled Specimen. From Fig. 7b, a fiber bundle adjacent to a poorly filled weave cavity. Partially crossed polarizers.

## IV. MESOPHASE STABILIZATION BY OXIDATION

The process of mesophase oxidation was initially studied in this program as a means of stabilizing the mesophase microstructures formed by deformation or by magnetic orientation. Such stabilization prevents microstructural disruption during carbonizing heat treatments. In the course of these studies, the oxidation process was found to have strong throwing power along access porosity formed by the anisotropic shrinkage of the mesophase. This observation was exploited in FY 85 to learn whether oxidation stabilization can be used as an alternative method of fixing a mesophase matrix in place within a 3D preform without the bloating inefficiencies of thermal hardening.

First we report on the completion of some elementary studies of mesophase oxidation and carbonization that were begun in FY 84; then we describe current studies of oxidation stabilization of the mesophase matrices of 3D composites.

### A. OXIDATION STABILIZATION OF DRAWN MESOPHASE RODS

The previous annual report[3] described micrographic observations of oxidation stabilization in mesophase rods produced by extrusion and draw. We restricted oxidation temperatures to 300°C or less to avoid coarsening of the fine fibrous microstructure of the drawn mesophase rod and found that this microstructure could be stabilized for carbonization to depths as great as 45 μm from any surface or crack with access to the oxidizing environment (usually $O_2$ in our experiments). This exploratory study has now been completed by obtaining the result illustrated in the lower part of Fig. 9. Using an oxidation temperature of 222°C (as suggested by the thermogravimetric results given below) and exposure to $O_2$ for 83 h, the fine fibrous microstructure was retained, after carbonization to 1000°C, to a depth of 70 μm.

Table 2 summarizes our observations of the stabilization depth in oxidized mesophase rods. Oxidation stabilization appears to be a diffusion-limited process, varying with oxygen pressure, temperature, and time, but also demonstrating strong throwing power in mesophase cracks. Depths of 70 μm may well be sufficient to stabilize the mesophase matrices of carbon-carbon

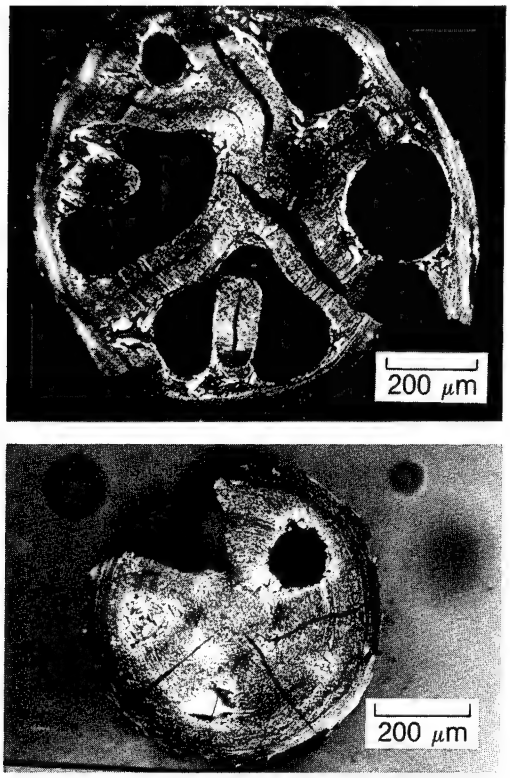


OXIDANT: $O_2$
TEMPERATURE: 265°C
DURATION: 64 h
STABILIZATION: 36 μm

OXIDANT: $O_2$
TEMPERATURE: 222°C
DURATION: 83 h
STABILIZATION: 70 μm

Figure 9. Oxidation Stabilization of Drawn Mesophase Rods. After carbonization of the oxidized rods, the stabilized region is revealed by the depth to which the original fine fibrous microstructure is retained relative to the free surface or to a crack with access to the oxygen atmosphere. Partially crossed polarizers.

Table 2. Depths of Stabilization by Mesophase Oxidation

| Mesophase Microstructure | Oxidant | Temperature (°C) | Time (h) | Depth (μm) |
|---|---|---|---|---|
| "Single crystal," by magnetic orientation | Air | 240 | 34 | 17 |
| Fine fibrous rods, by extrusion and draw | Air | 300 | 8 | 10 |
| | Air | 300 | 60 | 30 |
| | Oxygen | 300 | 64 | 45 |
| | Oxygen | 265 | 64 | 36 |
| | Oxygen | 222 | 83 | 70 |

composites, which display coarse crack structures between fiber bundles[16] and a finer crack structure within the bundles.[3]

## B. OXIDATION AND CARBONIZATION PROCESSES

Weight changes observed in some of the oxidation runs on mesophase rods evidenced that substantial quantities of oxygen were absorbed and that both weight-gain and weight-loss reactions were involved. The diffusion depths indicate that a complex response to time and temperature occurs in the range of 200 to 300°C. Accordingly, isothermal thermogravimetric (TGA) runs were made on the oxidation in $O_2$ of sized particles (-325/+400 mesh, 38 to 45 μm) of the mesophase pitch used to extrude and draw rods.

Some early results of this study were given in the previous annual report.[3] A more complete set of TGA oxidation curves over the temperature range 222 to 320°C, in Fig. 10a, presents a regular pattern consisting of rapid initial weight gains to about 11% that are subsequently overtaken by slower weight-loss reactions.

In view of the favorable carbonization behavior for the mesophase oxidized at lower temperatures (described below), four oxidation runs were made at 222°C under nominally equivalent conditions. The resulting curves in Fig. 10b show good reproducibility in shape although the range in weight gain is approximately 20%.

Thermogravimetric runs were made on carbonization of the oxidized mesophase particles in nitrogen to 1000°C at 10°C/min. The results are plotted in Fig. 11 with a carbonization yield curve for the unoxidized pitch for comparison. Oxidation stabilization at temperatures above 235°C exacts some loss in carbon yield, but temperatures below 235°C are beneficial, at least in terms of increasing carbon yield.

## C. OXIDATION STABILIZATION OF MESOPHASE-IMPREGNATED 3D PREFORMS

The foregoing results led to direct tests of oxidation stabilization on the mesophase-impregnated 3D specimens prepared by pressure cycling. A differential experiment was applied to two nominally equivalent specimens cut from the same impregnated preform. One specimen was oxidized, then both were

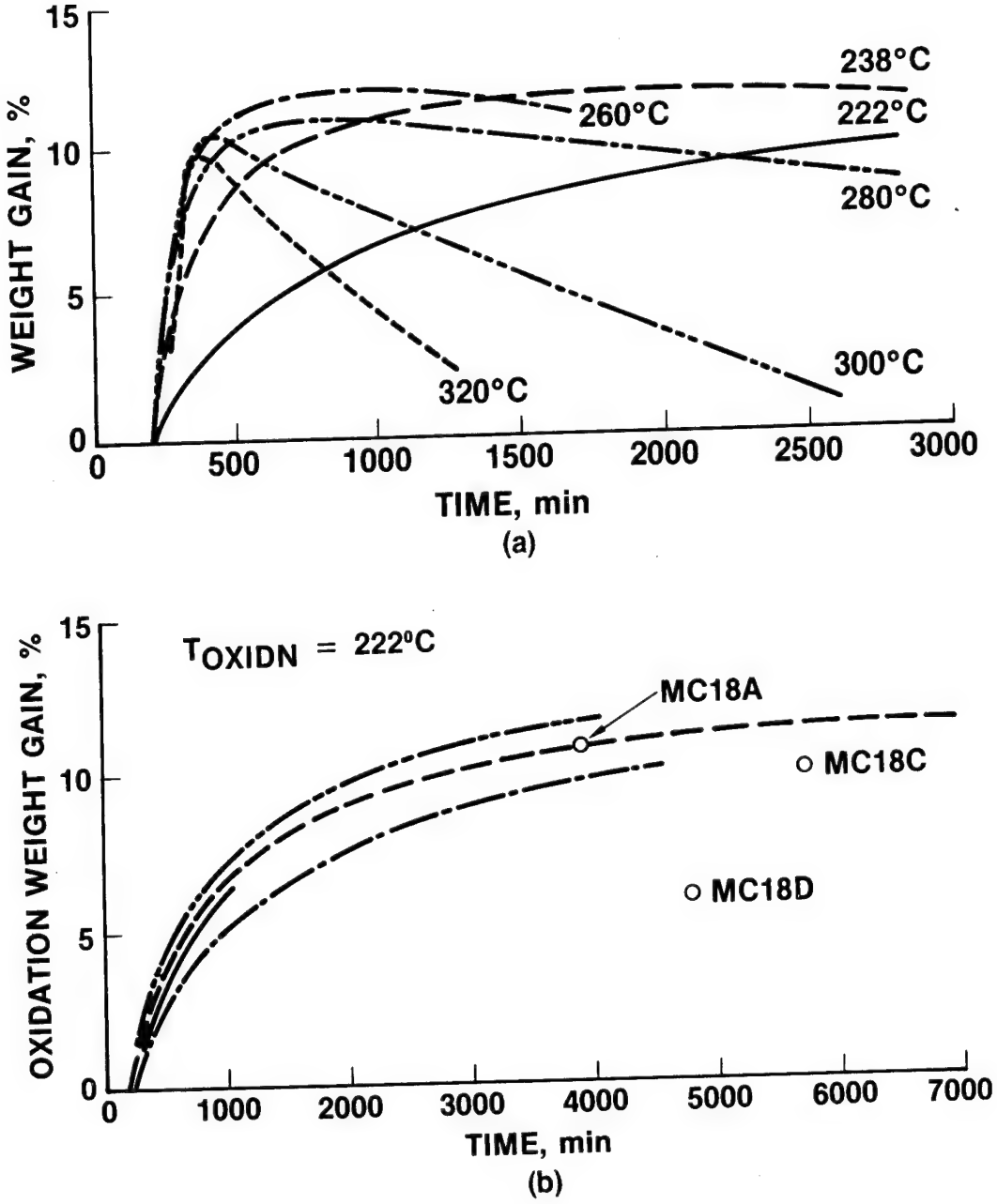


Figure 10. Oxidation of Mesophase Powder. TGA curves for the oxidation of particles, sized to -325/+400 mesh, in flowing $O_2$. The heating rate to reach the temperatures shown was 1°C/min, so the oxidation processes begin near 200-min exposure. The four curves at 222°C in (b) demonstrate the level of reproducibility and permit comparison of oxidation weight gains of 3D mesophase-impregnated preforms (indicated by labeled points).

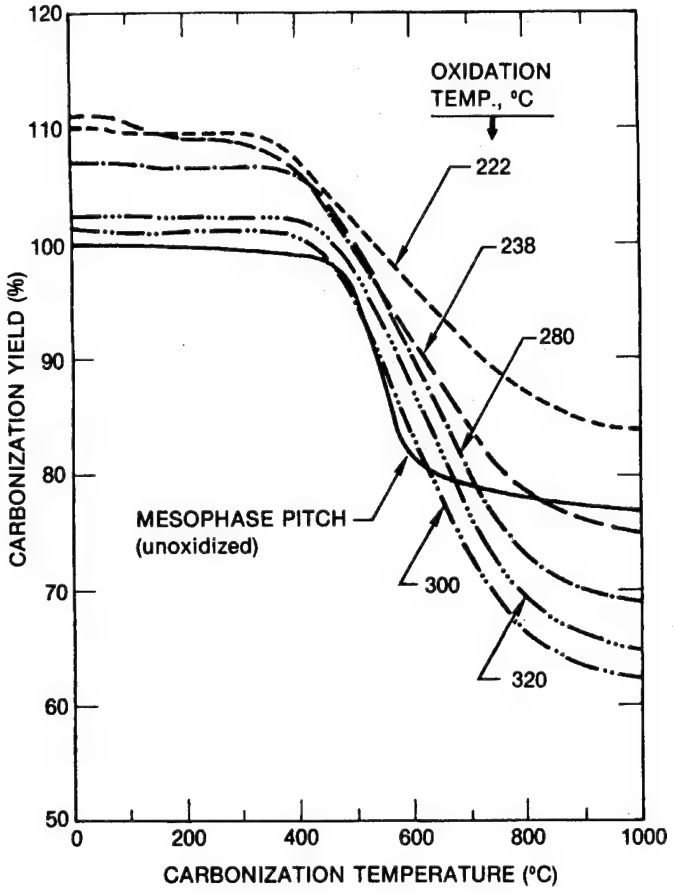


Figure 11. Carbonization of Oxidized Mesophase Powder. TGA curves for sized and oxidized particles carbonized in $N_2$ to 1000°C at 10°C/min. The carbonization yields are relative to the initial weights of mesophase pitch before oxidation and may be compared with the carbonization curve for the unoxidized mesophase pitch.

carbonized rapidly to 1200°C and examined to observe the stability of the mesophase in fiber bundles and weave cavities. For the initial experiments, 222°C was selected as the oxidation temperature, and the exposure times were about 4000 min.

The bulk test specimens were cut as pie-shaped blocks from the pressure-cycled cylinders, with radii and heights approximating 8 mm. One TGA run was made with a smaller, cube-shaped specimen approximately 3 mm on each side. Further details for the four oxidation-carbonization experiments are given in Table 3 with results for oxidation weight gains and carbonization yields.

Table 3. Oxidation and Carbonization Runs on 3D Mesophase-impregnated Preforms

| Preform Designation (Refer to Table 1) | | MC18A | MC18A | MC18C | MC18D |
|---|---|---|---|---|---|
| Specimen Type | | bulk | TGA | bulk | bulk |
| Specimen Weight | (mg) | 745 | 52 | 605 | 650 |
| Oxidation Run | | | | | |
| Temperature | (°C) | 222 | 222 | 222 | 222 |
| Duration | (min) | 3930 | 3840 | 5760 | 4800 |
| Composite Weight Gain | (%) | 3.07 | 3.17 | 4.36 | 2.46 |
| Matrix Weight Gain | (%) | 10.70 | 11.05 | 9.87 | 5.84 |
| Carbonization Run | | | | | |
| Maximum Temperature | (°C) | 1200 | 1000 | 1200 | 1200 |
| Heating Rate | (°C/min) | 10 | 10 | 6.7 | 6.7 |
| Weight Loss | (%) | 7.78 | 7.66 | Note a | Note a |
| Overall Yield (Note b) | (%) | 95.05 | 95.27 | ND | ND |
| Yield, Unoxidized Specimen | (%) | 95.07 | ND | Note a | Note a |

ND = Not determined.

NOTES:

[a]Exudation of matrix interfered with measurement of carbonization yield. Exudation was substantially greater for unoxidized specimens.

[b]Overall yield = (oxidation yield) × (carbonization yield).

The first two experiments, one a bulk oxidation test and the other a TGA sequence, were run on specimens cut from the mesophase-impregnated cylinder MC18A, which was the lowest-density specimen from the pressure-cycled series. The results, summarized graphically in Fig. 12, show that, despite the difference in size of TGA and bulk specimens, the oxidation weight gains were in good agreement and close to the weight gain for mesophase powder. A TGA curve for the mesophase powder, adjusted to the matrix fraction of the impregnated preform, is included in Fig. 12 to show that, in the early stages of oxidation ($t < 200$ min), the impregnated preform oxidized more rapidly than the mesophase powder.

In the carbonization runs, the bulk and TGA specimens were also in good agreement, and their weight loss followed a pattern similar to that for oxidized mesophase powder. No exudation of matrix during carbonization was observed for either the oxidized or reference specimens. Although the state of pyrolysis in the preparation of this impregnated cylinder was sufficiently advanced that stabilization was apparently unnecessary, the access porosity was adequate for oxidation to proceed in the specimen, without delay, to near-saturation levels. Indeed, the enhanced oxidation rate in the early stages suggests that the matrix has developed a more effective access porosity than was present in the crushed mesophase powder. Two possible mechanisms for porosity introduction are fracturing due to thermal contraction differences between fiber and mesophase and fracturing due to damage imposed by cutting the specimens when the mesophase is quite fragile. Although the latter mechanism is probably limited to a depth of about 1 mm, it could account for the advanced oxidation rate for the 3-mm specimen used in obtaining the TGA data in Fig. 12a.

The third stabilization experiment was run on pressure-cycled specimen MC18C, the matrix of which had been only partially transformed to mesophase. As indicated in Fig. 10b, the matrix weight gain of 9.87% in oxidation at 222°C was near to that for the mesophase powder. However, upon carbonization, this specimen exuded small amounts of matrix, indicating that further oxidation is required for full stabilization of a partially transformed matrix. Micrographs on the carbonized specimens are presented at three levels of magnification for comparison, in Figs. 13 to 15. At all magnification levels,

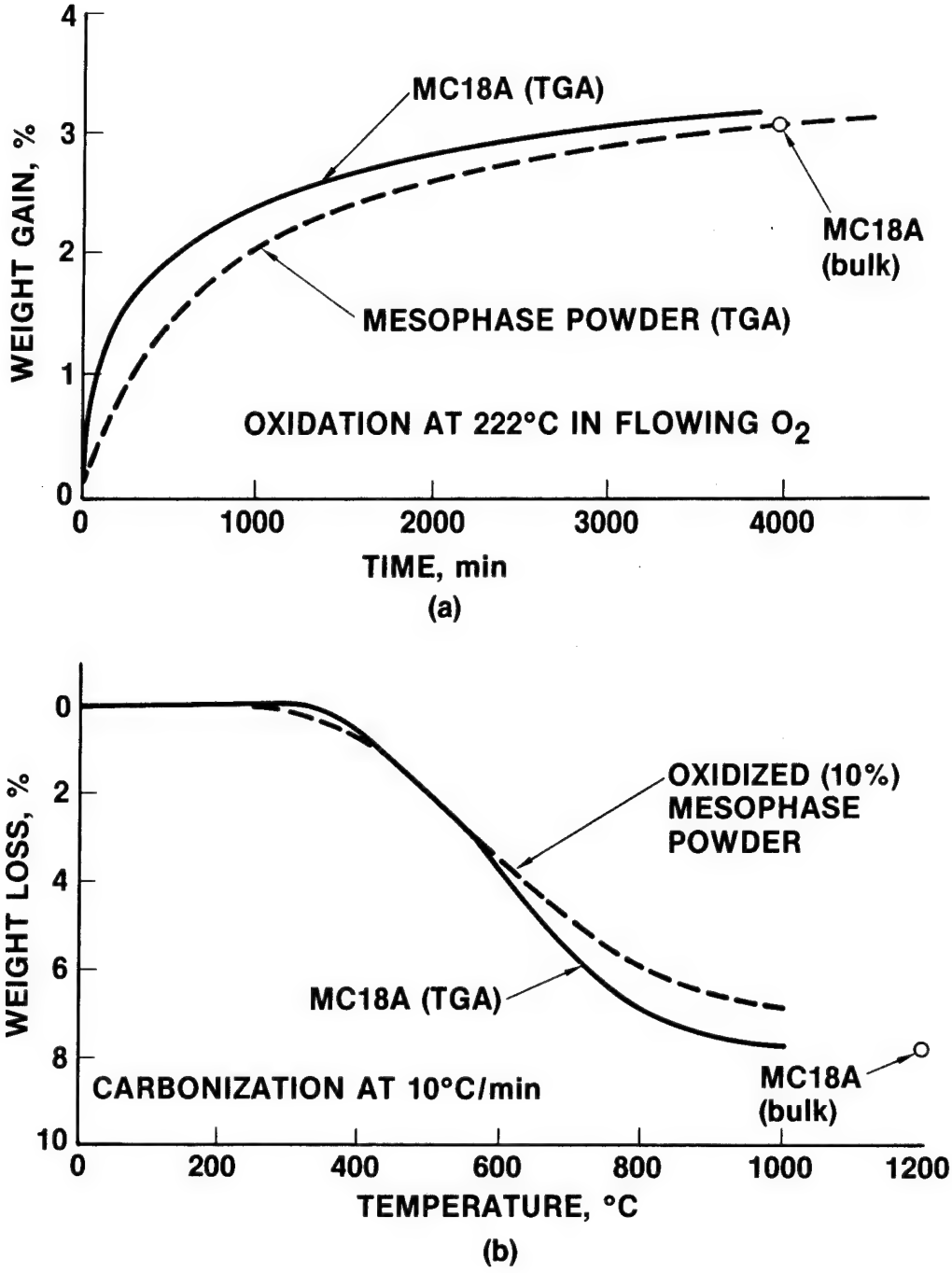


Figure 12. Oxidation and Carbonization Runs on a Mesophase-impregnated 3D Preform. Specimens from experiment MC18A plotted for comparison with TGA runs on mesophase powder (weight-change curves adjusted to the mesophase content of the composite).

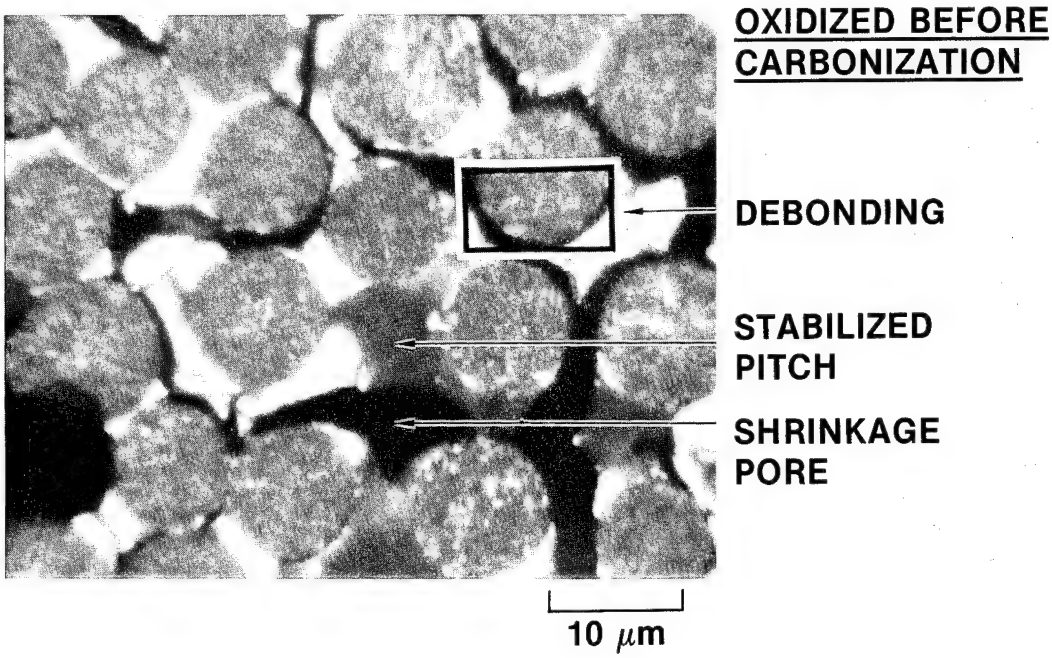


Figure 13. Microstructures of Mesophase-impregnated 3D Composites after Carbonization. Low-magnification views of specimens from pressure-cycling experiment MC18C. Top: carbonized after oxidation; pools of isotropic pitch are retained in weave cavities. Bottom: carbonized without oxidation; new porosity has formed in fiber bundles and weave cavities. Crossed polarizers.

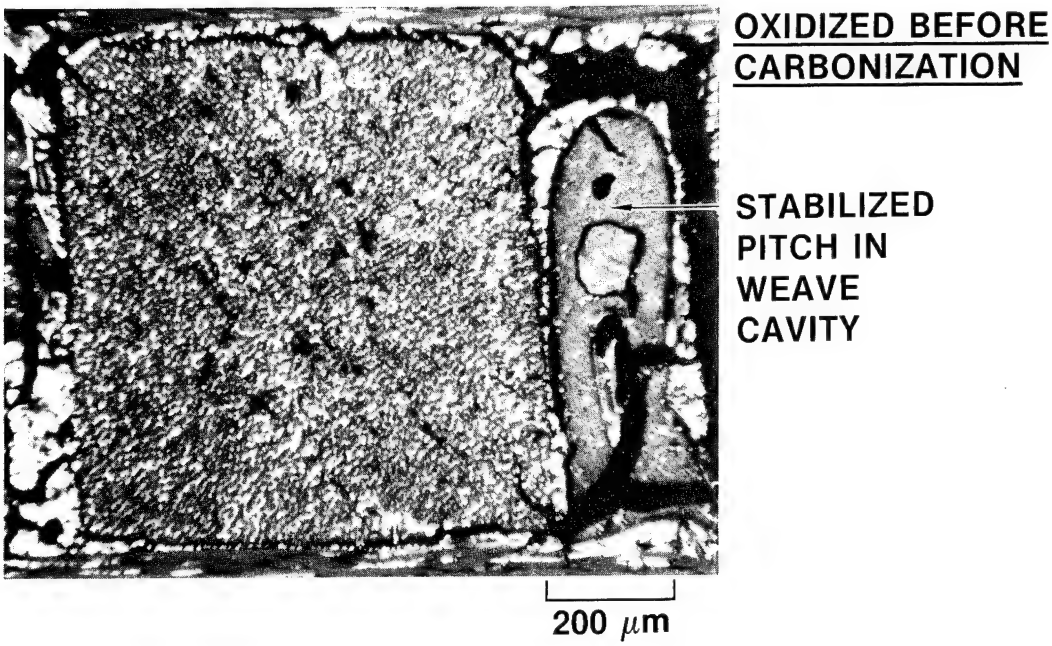


Figure 14. Microstructures of Mesophase-impregnated Fiber Bundles after Carbonization. Moderate-magnification views of specimens in Fig. 13. Top: carbonized after oxidation; mesophase spherules are retained in pitch pools; crossed polarizers. Bottom: carbonized without oxidation; polarizer only.

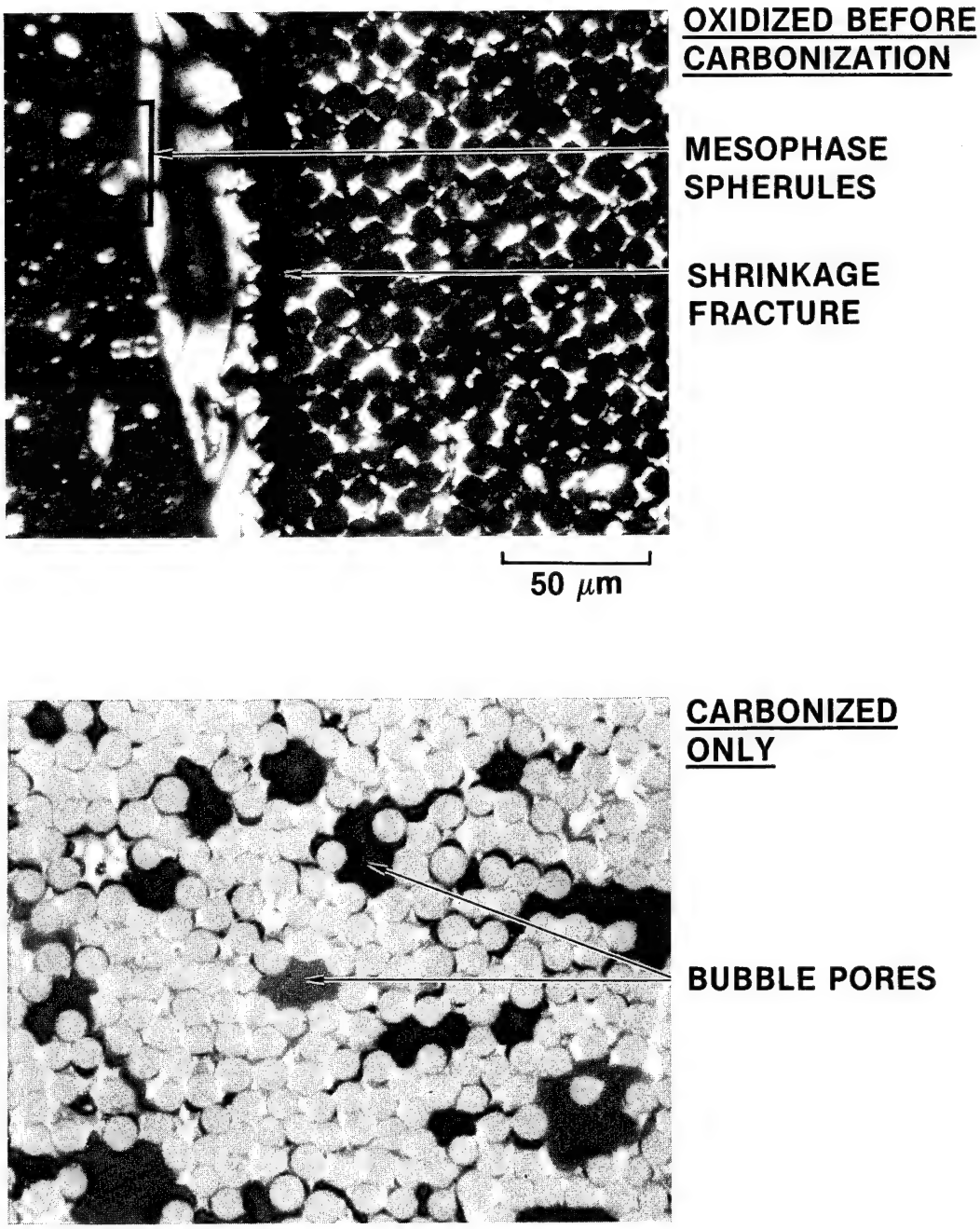


Figure 15. Microstructures of Mesophase Matrices after Carbonization. High-magnification views of specimens in Figs. 13 and 14: Top: carbonized after oxidation; mesophase-pitch wetting conditions are retained; crossed polarizers, oil immersion. Bottom: carbonized without oxidation; polarizer only. Oil immersion.

it is clear that oxidation has stabilized both mesophase and pitch. In Fig. 14, Brooks-and-Taylor spherules are clearly evident immersed in the pitch phase of the oxidized and carbonized specimen. The unoxidized specimen has developed appreciable porosity in the fiber bundles and in the weave cavities; the pores in the fiber bundles show transverse dimensions of the order of 20 μm.

The micrographs of Fig. 15, taken near the limit of optical resolution, show that roughly equivalent shrinkage cracking is in progress in such carbonized specimens, while oxidation has preserved the mesophase-pitch wetting and alignment geometry illustrated schematically in Figs. 2 and 3.

The fourth stabilization experiment was run on pressure-cycled specimen MC18D, which was well impregnated with a matrix approaching complete transformation to mesophase. The oxidation level (5.84% weight gain relative to matrix content) falls short of the level attained with the mesophase powder. Upon carbonization, some matrix was exuded from the oxidized composite, although much less than appeared on the unoxidized composite. However, as illustrated by the micrographs of Figs. 16 to 18, the oxidized specimen exhibits good retention of mesophase in weave cavities and less porosity in the fiber bundles. There appear to be no distinctions in carbonization mechanisms operating within the mesophase matrix or at the fiber-matrix interface, in the high-resolution micrographs of Fig. 18, between the oxidized and unoxidized specimens.

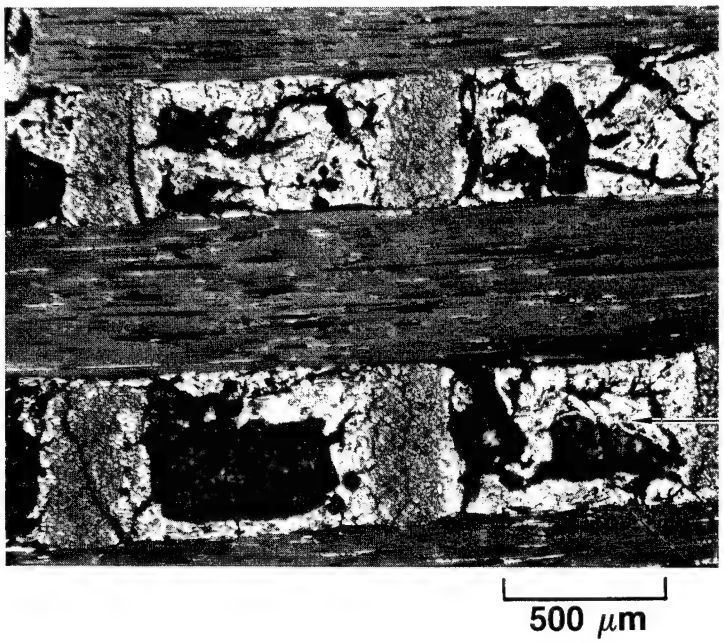


Figure 16. Microstructures of Mesophase-impregnated 3D Composites after Carbonization. Low-magnification views of specimens from pressure-cycling experiment MC18D. Top: carbonized after oxidation; appreciable mesophase is retained in weave cavities. Bottom: carbonized without oxidation; little mesophase retained in weave cavities. Partially crossed polarizers.

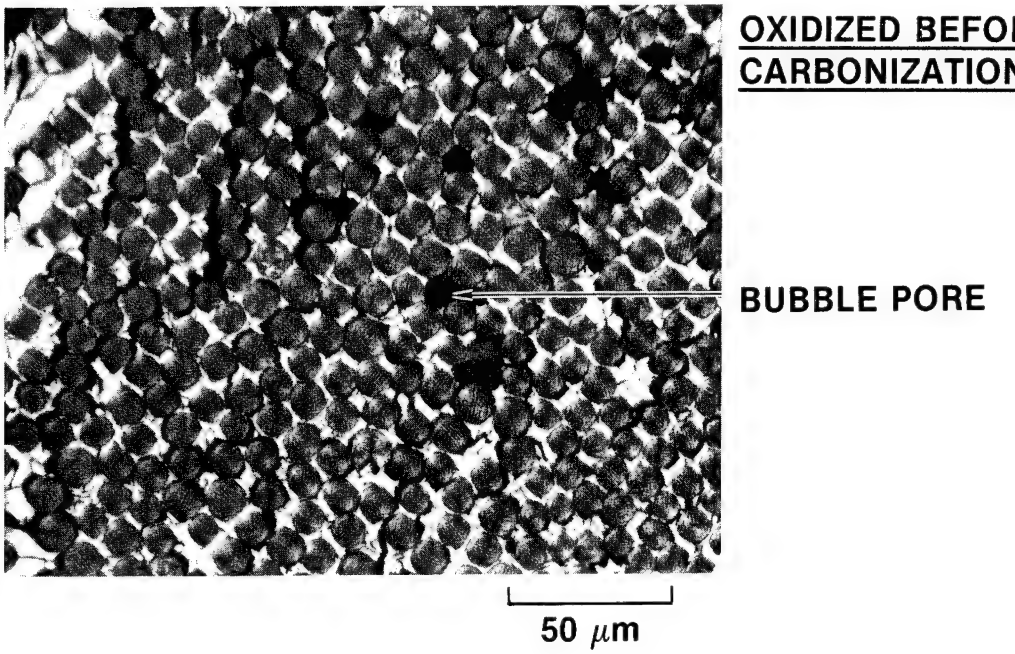


Figure 17. Microstructures of Mesophase-impregnated Fiber Bundles after Carbonization. Moderate-magnification views of specimens in Fig. 16. Top: carbonized after oxidation. Bottom: carbonized without oxidation. Partially crossed polarizers.

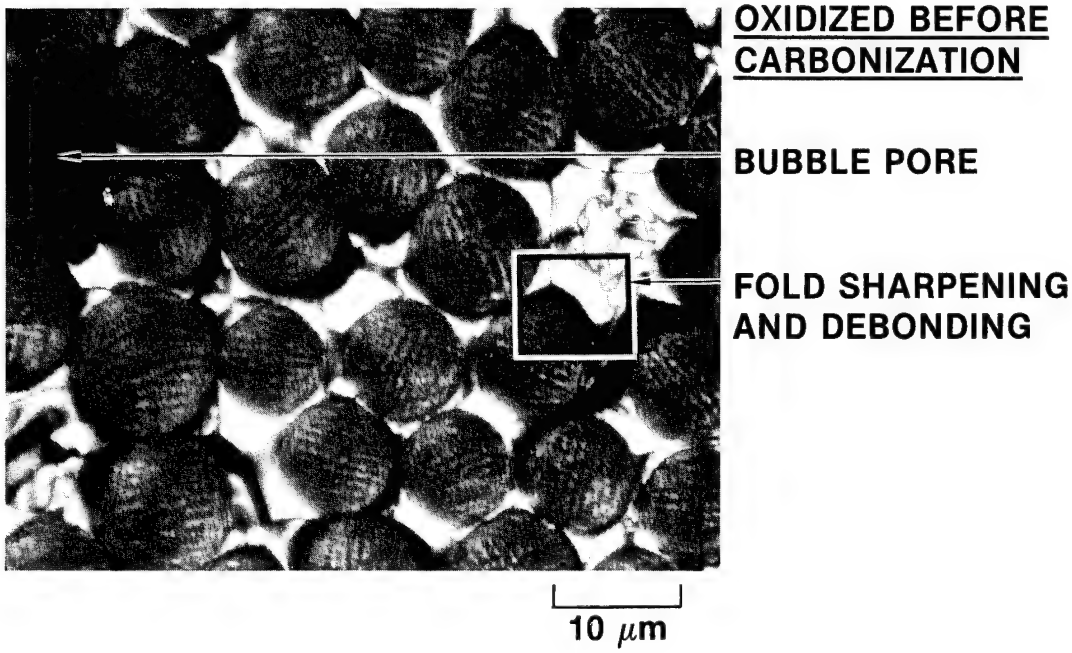


Figure 18. Microstructures of Mesophase Matrices after Carbonization. High-magnification views of specimens in Figs. 16 and 17. Top: carbonized after oxidation. Bottom: carbonized without oxidation. Partially crossed polarizers, oil immersion.

## V. EFFECTS OF HEAT TREATMENT ON MESOPHASE MATRICES

The effects of heat treatment on mesophase microstructure begin essentially from the point of hardening to a liquid-crystalline glass near 500°C and extend to graphitization temperatures above 3000°C.[17] The micrographs of Fig. 19 are of bulk mesophase formed from an extracted coal-tar pitch and illustrate several microstructural processes that are expected to play important roles in composite processing and properties:

- Anisotropic shrinkage to form lenticular cracks.
- Changes in layer curvature to give "fold-sharpening," i.e., the localization of layer curvature to a single fold that resembles a twin boundary.[17]
- Local distortions, including rotations and displacements, sufficient to cause layer ruptures.
- Kinking and local ordering that appear as fine structures in the final stages of thermal graphitization.[17]

Although all of the mechanisms clearly relate to the general process of graphitization, little work has been done to define the specific mechanisms involved in the thermal conversion of the liquid-crystalline mesophase glass to crystalline graphite. Local mesophase distortions occur in all the mechanisms, so their action within the matrix of a fiber bundle may significantly affect fiber-matrix bonding and filament utilization. We have undertaken a study of singly impregnated fiber bundles and 3D preforms at specific levels of heat treatment to learn how such distortion mechanisms act within fiber bundles.

Our observations began with the unidirectional composite consisting of VSA-11 mesophase pitch fiber impregnated with A240 petroleum pitch and heat-treated under inert atmosphere to 1680°C (Fig. 20). In the fiber bundle, the mesophase distortions operate on the scale of the sheaths imposed by filament diameters and spacing (see Fig. 3), but are otherwise similar to those appearing in bulk mesophase. Debonding and shrinkage cracking are extensive. At the resolution available to optical microscopy, a tendency toward adhesive

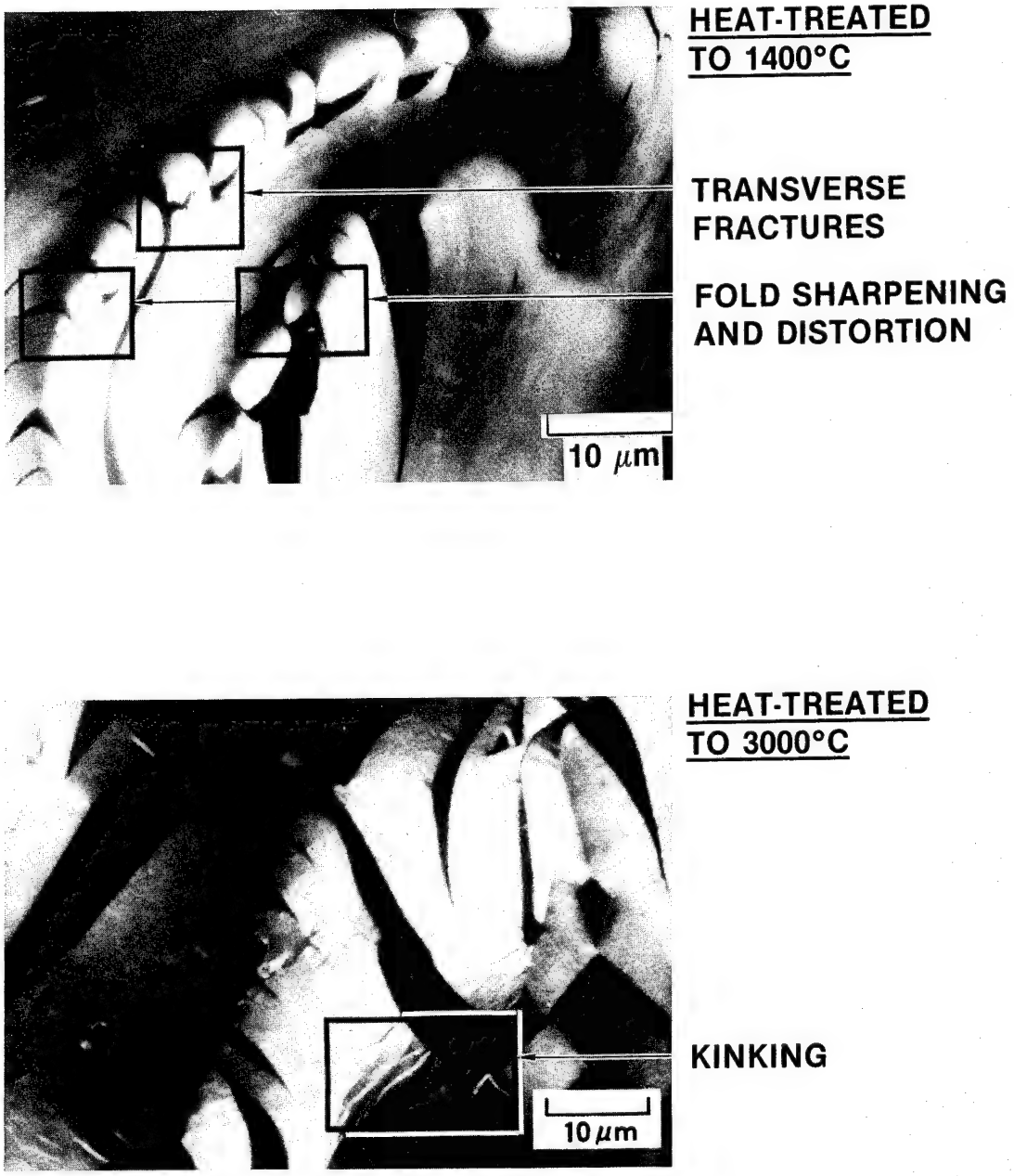


Figure 19. Effects of Heat Treatment on Mesophase Microstructures. Mesophase produced by pyrolysis of a coal-tar pitch treated by solvent-extraction to remove insoluble particles. Polarizer only, oil immersion. From Ref. 17.

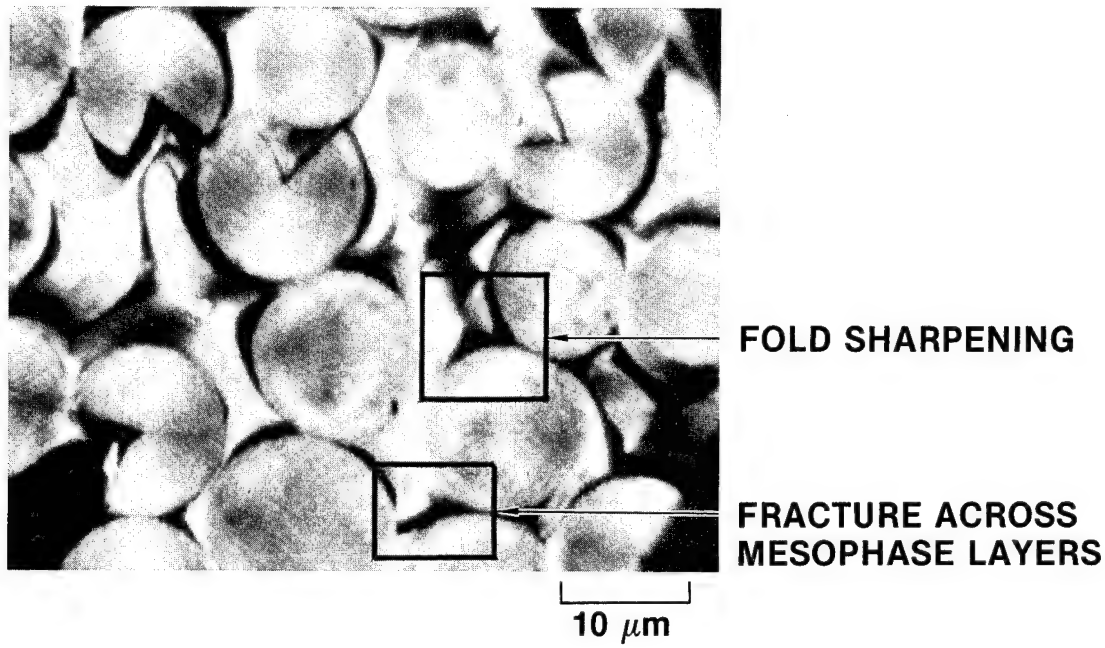


Figure 20. Mesophase Shrinkage, Distortion, and Debonding from Filaments in a Fiber Bundle Heat-treated to 1680°C. Transverse views of a unidirectional composite prepared by high-pressure pyrolysis of VSA-11 mesophase carbon fiber impregnated with A240 petroleum pitch. Polarized light, oil immersion.

failure is noted. The curvatures in the mesophase sheath are not stable under thermal treatment; fold sharpening proceeds to produce debonding, sometimes in a regular pattern around circular filaments. The local distortions can be substantial relative to the size of matrix channels, and local stresses in the matrix are sufficient to cause some layer ruptures (fractures running across layer planes) and occasionally to split open-wedge filaments. Inspection of the higher-magnification micrographs given in the section on oxidation stabilization (Figs. 15 and 18) reveals that these microstructural processes are also active at 1200°C.

The present observations, on singly impregnated bundles and preforms, are consistent with the concepts in Jortner's[18] proposed model for the tensile fracture of fiber bundles: that the fiber-matrix interface is weak and that load transfer occurs primarily by friction. Our observations contribute the following detail that may be important to understanding fiber utilization: The mesophase sleeve around each filament, while generally presenting the graphitic layer plane to the fiber surface, is not a smooth, cylindrical sheath but appears to be distorted along the lines indicated in Fig. 21. Filament-matrix load transfer must then take place by many local contacts, some of which apply forces sufficient to split open-wedge filaments.

The poor fiber utilization factors observed after the first densification cycle[12] may be accounted for by the extensive fiber-matrix debonding, with resulting long stress-transfer lengths and combined with the irregular locations of local contact. Subsequent cycles of impregnation and heat treatment tend to fill the slit-shaped pores between filament and matrix, thus tightening and smoothing the matrix sleeve; both effects should contribute to the improved utilization factors that are, in fact, observed. Nevertheless, a question remains as to how far such slit-filling and sleeve-smoothing can make up for the matrix distortions introduced in the first densification cycle.

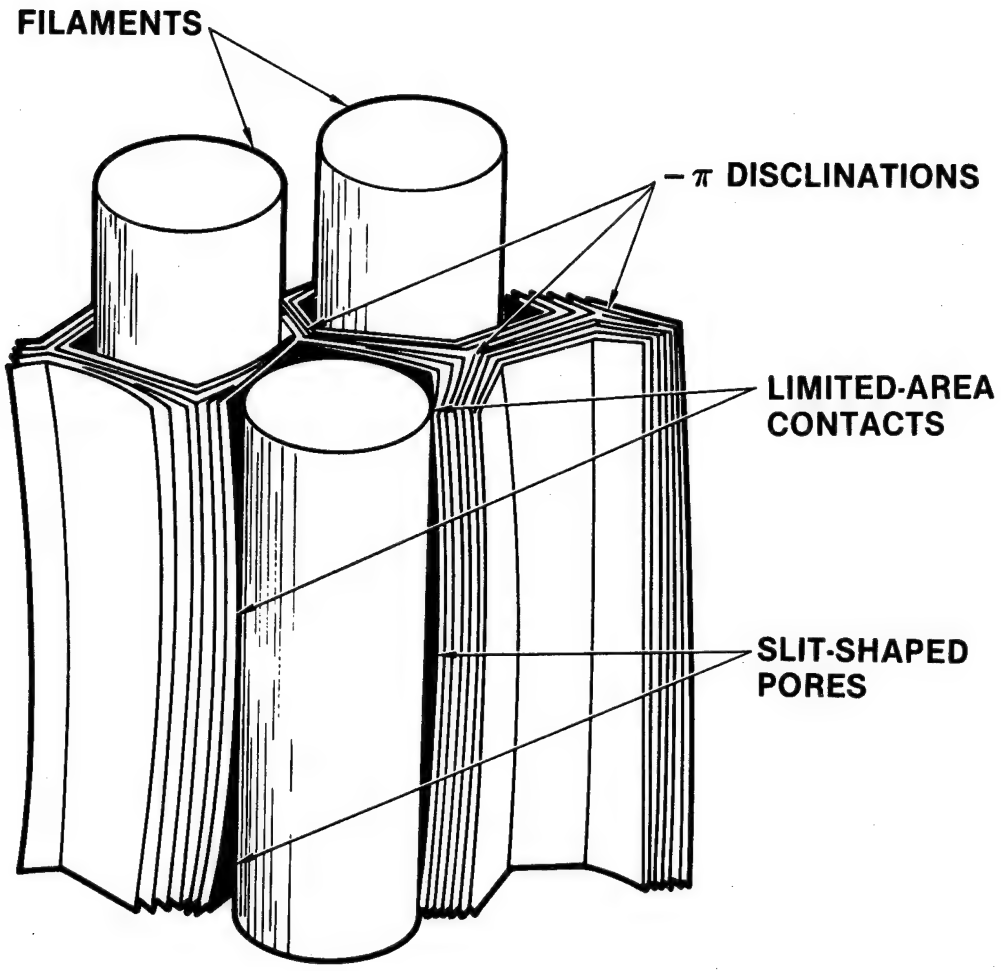


Figure 21. Schematic Diagram of Matrix Distortions in a Fiber Bundle. Heat treatment activates fold sharpening and mesophase distortions that cause debonding and the formation of localized regions of load transfer separated by faceted slits around each filament.

# VI. DISCUSSION

## A. MATRIX MICROSTRUCTURES

The wetting and alignment conditions illustrated in Figs. 2 and 3 were strikingly consistent for the range of fibers and other variables studied. These and other aspects of mesophase behavior that relate to the formation of matrix microstructure while the mesophase is fluid, or at least deformable, are summarized in Table 4. They establish a useful level of predictability that may reasonably be expected to apply to mesophase-forming precursors in general. However, one important and unpredictable factor is the bubble porosity, which depends on the amount of pyrolysis gas formed as the matrix viscosity rises to fix the mesophase in place within the composite.

Table 4. Summary: Mesophase Formation in Composite Processing

FORMATION OF MATRIX MICROSTRUCTURE

- MESOPHASE ALIGNMENT ("sheath effect") IS THE DOMINANT MECHANISM
- FIBERS ARE WET BY BOTH PITCH AND MESOPHASE
- MICROSTRUCTURE FORMATION IS SIMILAR FOR ALL FIBER TYPES
- MATRIX BLOATING REDUCES IMPREGNATION EFFICIENCY
- MATRIX HETEROGENEITIES CAN FORM
- COOLING PRODUCES EXTENSIVE FRACTURING IN MESOPHASE

EFFECTS OF HIGH-PRESSURE PYROLYSIS (15 kpsi)

- MICROSTRUCTURES ARE PREDICTABLE FROM ROOM-PRESSURE PYROLYSIS
- MESOPHASE TRANSFORMATION AND HARDENING ARE RETARDED SLIGHTLY
- MATRIX BLOATING IS STILL ACTIVE

At least several mechanisms act to produce matrix distortions and extensive debonding from filaments, according to our initial observations of the effects of heat treatment on the mesophase microstructures, from the point of hardening to graphitizing temperatures. In further work, these observations should be extended to wider ranges of temperature and to reimpregnated bodies. In seeking to understand the mechanisms of distortion and crack formation, it may be necessary to look beyond anisotropic-shrinkage mechanisms in a multiply connected body to consider the role of chemical segregation that may occur during the mesophase transformation. If heterogeneous layers are deposited during transformation, distortions may reasonably be anticipated, owing to the varied response of the layers to heat treatment.

In modeling the mechanical and thermal properties of carbon-carbon composites, Jortner[18] has adopted the concept that load transfer between filament and matrix is primarily frictional. The model of a strong, stiff filament free to slip frictionally in a matrix sleeve is consistent with our observations of mesophase alignment and debonding but also implies that load transfer, and perhaps fiber strength, will depend on matrix distortions. To respond to Jortner's call for quantitative experimental data to test and develop the frictional model, we note that single-filament tensile testing should be applicable to filament pullout experiments, provided that a suitable specimen can be fabricated, e.g., by incorporating filaments of known immersion depth at the end of a well-defined bundle that can be filled with pitch by wicking. The geometrical requirements for the pullout specimens are greatly eased by the expectation that stress-transfer distances are large.

## B. COMPOSITE PROCESSING

In the work on pressure-cycling, we demonstrated that the mesophase can be moved within the preform by hydraulic pressures that are feasible in composite processing, and that appreciable improvements in mesophase impregnation can be realized. However, the processing window between mesophase formation and hardening is small, at least for mesophase pitch formed by pyrolysis of A240 petroleum pitch. Thus, some points to address in further work are better definition of the pyrolysis treatment desired prior to pressure cycling and

exploration of the pressure-cycling variables to identify to what levels the porosity can be reduced. Consideration should also be given to mesophase precursors that produce more fluid mesophase and evolve less gas during pressure cycling.

As applied to the mesophase-impregnated specimens tested thus far, the process of oxidation stabilization appears feasible. Although full stabilization throughout the body has not yet been demonstrated, the oxygen levels attained suggest that full stabilization can be achieved by extending the exposure time. However, the process is clearly dependent on access porosity, which may decrease or become more tortuous as more fully impregnated composites are tested. Since the access porosity is believed to result from the thermal expansion difference between fiber and matrix,[16] and the thermal expansion of mesophase varies rapidly as pyrolysis reactions cause mesophase hardening,[19] consideration of adequate access porosity may enter the choice of pyrolysis state for pressure cycling.

Finally, a cautionary note should be made on the heat treatment required to convert oxygen-stabilized mesophase to graphitizable carbon. Oxidation stabilization appears to work well when applied to carbon fiber in diameters of about 10 μm, but the oxygen levels that we find necessary for bulk mesophase are high, and questions arise concerning the release of oxygen without damage to matrix or fiber during heat treatment. At this point we can only note that the microstructures of oxidized and unoxidized composites, observed optically after carbonization to 1200°C (see Figs. 13-18), show no significant differences. Ultimately the extent of fiber degradation during oxidation and carbonization must be resolved by mechanical testing.

## VII. REPORTS, PUBLICATIONS, AND PRESENTATIONS

The last annual report[3] included a list of reports, publications, and presentations resulting from or prepared with support from this research program. The following is an update of that list, with full references where available, and includes new items prepared or presented in FY 85.

- J. L. White and P. M. Sheaffer, Mesophase Behavior Fundamental to the Processing of Carbon-Carbon Composites, TOR-0084A(5728-01)-4, The Aerospace Corporation, El Segundo, California (March 1985); interim technical report on this program for 1 October 1983 through 30 September 1984.

- G. W. Smith, J. L. White, and M. Buechler, "Mesophase/Isotropic Phase Interfacial Energy: Determination from Droplet Coalescence Kinetics," Ext. Abstr., 17th Conf. Carbon (1985), pp. 163-64; a collaborative paper with G. W. Smith of General Motors Research Laboratory, Warren, Michigan.

- J. D. Bacha, J. W. Newman, and J. L. White, eds., Petroleum-Derived Carbons, Am. Chem. Soc. Symp. Series, 303, April 1986, 406 pages with index; cloth, ISBN 0-8412-0964-2; proceedings of an ACS Symposium held in St. Louis, Missouri, in April 1984.

- J. L. White and M. Buechler, "Microstructure Formation in Mesophase Carbon Fibers and Other Graphitic Materials," in Petroleum-Derived Carbons, Am. Chem. Soc. Symp. Series, 303 (1986), pp. 62-84; contribution to book described in foregoing entry.

- J. L. White and P. M. Sheaffer, "Mesophase Formation within Fiber Bundles and 3D Fiber Preforms," paper presented at 1985 JANNAF Rocket Nozzle Technology Subcommittee Meeting, Naval Postgraduate School, Monterey, California (November 1985); submitted for publication.

## REFERENCES


1. J. L. White, TR-0083(3728-01)-1, The Aerospace Corporation, El Segundo, California (December 1982).

2. J. L. White and P. M. Sheaffer, TR-0084(4728-01)-2, The Aerospace Corporation, El Segundo, California (December 1983).

3. J. L. White and P. M. Sheaffer, TOR-0084A(5728-01)-1, The Aerospace Corporation, El Segundo, California (March 1985).

4. J. L. White and P. M. Sheaffer, 1985 JANNAF Rocket Nozzle Technology Subcommittee Meeting, U.S. Naval Postgraduate School, Monterey, California (November 1985), in press.

5. J. E. Zimmer and J. L. White, Carbon 21, 323 (1983).

6. J. D. Brooks and G. H. Taylor, Carbon 3, 185 (1965).

7. J. E. Zimmer and R. L. Weitz, Carbone 84. Extended Abstracts for French Carbon Conf. (1984), p. 386.

8. J. E. Zimmer and J. L. White, Adv. Liq. Cryst. 5, 157 (1982).

9. J. L. White and M. Buechler, Petroleum-Derived Carbons, Am. Chem. Soc. Symp. Series 303, 62 (1986).

10. J. S. Evangelides and R. A. Meyer, TR-0084(4645-02)-1, The Aerospace Corporation, El Segundo, California (July 1984).

11. J. L. White, Petroleum-Derived Carbons, Am. Chem. Soc. Symp. Series 21, 282 (1976).

12. E. Fitzer and A. Gkogkidis, Am. Chem. Soc. Symp. Series 303, 346 (1986).

13. H. Brückmann, Dr.-Ing. Thesis, University of Karlsruhe (1979).

14. R. A. Meyer et al., TOR-0084(4726-08)-1, The Aerospace Corporation, El Segundo, California (February 1984).

15. R. W. Seibold, D. L. Kinney, and P. C. Hopkins, MDC G7878, McDonnell Douglas Astronautics Co., Huntington Beach, California (January 1979).

16. J. Jortner, Ext. Abstr., 13th Conf. Carbon (1977), p. 406.

17. J. L. White, Prog. Solid State Chem. 9, 59 (1973).

18. J. Jortner, 1984 JANNAF Rocket Nozzle Technology Subcommittee Meeting, Marshall Space Flight Center, Huntsville, Alabama, CPIA Publication 416 (December 1984), p. 275.

19. J. E. Zimmer and J. L. White, Ext. Abstr., 13th Conf. Carbon (1977), p. 318.